

Membrane-Tethered Metalloproteinase Expressed by Vascular Smooth Muscle Cells Limits the Progression of Proliferative Atherosclerotic Lesions

Richard H. Barnes, II, BS; Takeshi Akama, PhD; Miina K. Öhman, MD, PhD; Moon-Sook Woo, PhD; Julian Bahr, BS; Stephen J. Weiss, MD; Daniel T. Eitzman, MD; Tae-Hwa Chun, MD, PhD

Background—The MMP (matrix metalloproteinase) family plays diverse and critical roles in directing vascular wall remodeling in atherosclerosis. Unlike secreted-type MMPs, a member of the membrane-type MMP family, MT1-MMP (membrane-type 1 MMP; MMP14), mediates pericellular extracellular matrix degradation that is indispensable for maintaining physiological extracellular matrix homeostasis. However, given the premature mortality exhibited by MT1-MMP-null mice, the potential role of the proteinase in atherogenesis remains elusive. We sought to determine the effects of both MT1-MMP heterozygosity and tissue-specific gene targeting on atherogenesis in APOE (apolipoprotein E)-null mice.

Methods and Results—MT1-MMP heterozygosity in the APOE-null background (*Mmp14*^{+/-}*ApoE*^{-/-}) significantly promoted atherogenesis relative to *Mmp14*^{+/+}*ApoE*^{-/-} mice. Furthermore, the tissue-specific deletion of MT1-MMP from vascular smooth muscle cells (VSMCs) in SM22 α -Cre(+)*Mmp14*^{F/F}*ApoE*^{-/-} (VSMC-knockout) mice likewise increased the severity of atherosclerotic lesions. Although VSMC-knockout mice also developed progressive atherosclerotic aneurysms in their iliac arteries, macrophage- and adipose-specific MT1-MMP-knockout mice did not display this sensitized phenotype. In VSMC-knockout mice, atherosclerotic lesions were populated by hyperproliferating VSMCs (smooth muscle actin- and Ki67-double-positive cells) that were characterized by a proinflammatory gene expression profile. Finally, MT1-MMP-null VSMCs cultured in a 3-dimensional spheroid model system designed to mimic in vivo-like cell-cell and cell-extracellular matrix interactions, likewise displayed markedly increased proliferative potential.

Conclusions—MT1-MMP expressed by VSMCs plays a key role in limiting the progression of atherosclerosis in APOE-null mice by regulating proliferative responses and inhibiting the deterioration of VSMC function in atherogenic vascular walls. (*J Am Heart Assoc.* 2017;6:e003693. DOI: 10.1161/JAHA.116.003693.)

Key Words: aneurysm • atherosclerosis • inflammation • matrix metalloproteinases • muscle • smooth

Vascular smooth muscle cells (VSMCs) constitute the major cellular component of the tunica media, where they play key roles in regulating vascular tone and blood

flow.¹ Under physiological conditions, the number of VSMCs within the arterial wall is tightly controlled, as is arterial wall thickness.^{1,2} In marked contrast, during the progression of atherosclerosis, VSMCs proliferate and transition from a contractile to a synthetic phenotype, thereby depositing excess extracellular matrix (ECM) molecules that lead to arterial wall thickening and stiffening, namely, arteriosclerosis.^{3,4} However, the molecular mechanisms that underlie VSMC proliferation and arteriosclerosis during the pathological process of atherosclerosis remain largely undefined.

ECM remodeling is mediated by members of the MMP (matrix metalloproteinase) gene family, a group of structurally related proteolytic enzymes that are broadly characterized as either secreted or membrane tethered.⁵ Consistent with their potential roles in vascular wall pathology, recent studies have characterized the roles of secreted MMPs, particularly MMP-2, MMP-8, and MMP-13, in promoting atherogenesis or plaque rupture.⁶⁻⁸ With regard to the membrane-tethered MMPs, MT1-MMP uniquely serves as a pericellular collagenase that

From the Division of Metabolism, Endocrinology and Diabetes, Department of Internal Medicine, University of Michigan Medical School, Ann Arbor, MI (R.H.B., T.A., M.-S.W., T.-H.C.); Biointerfaces Institute (R.H.B., T.A., M.-S.W., T.-H.C.), Department of Internal Medicine, Cardiovascular Research Center (M.K.Ö., D.T.E.), and Life Sciences Institute (J.B., S.J.W.), University of Michigan, Ann Arbor, MI.

Accompanying Table S1 and Figures S1, S2 are available at <http://jaha.ahajournals.org/content/6/7/e003693/DC1/embed/inline-supplementary-material-1.pdf>

Correspondence to: Tae-Hwa Chun, MD, PhD, NCRC B10-A186, 2800 Plymouth Rd, Ann Arbor, MI 48109. E-mail: taehwa@umich.edu

Received April 20, 2017; accepted June 8, 2017.

© 2017 The Authors. Published on behalf of the American Heart Association, Inc., by Wiley. This is an open access article under the terms of the Creative Commons Attribution-NonCommercial-NoDerivs License, which permits use and distribution in any medium, provided the original work is properly cited, the use is non-commercial and no modifications or adaptations are made.

Clinical Perspective

What Is New?

- The molecular mechanisms underlying proliferative atherosclerosis have not been fully defined.
- This animal study suggests that a pericellular collagenase called MT1-MMP (membrane-type 1 matrix metalloproteinase), expressed by vascular smooth muscle cells, plays a critical role in limiting the progression of proliferative atherosclerotic lesions.
- The loss of vascular smooth muscle cell MT1-MMP leads to advanced proliferative atherosclerosis and atherosclerotic iliac artery aneurysm formation.

What Are the Clinical Implications?

- The functional impairment of vascular smooth muscle cells in regulating vascular wall extracellular matrix remodeling may contribute to the pathogenesis of proliferative atherosclerosis and atherosclerotic iliac artery aneurysm formation.

cleaves native, triple-helical collagens associated with both the basement membrane and interstitial matrix.⁹ Indeed, in contrast to almost all other MMP family members, in which gene targeting exerts only minor effects on mouse development, MT1-MMP–knockout animals display severe dwarfism, lipodystrophy, and premature lethality, underscoring the key roles played by MT1-MMP in maintaining tissue homeostasis.^{10–12} Given the premature lethality of MT1-MMP–knockout mice, however, attempts to characterize the role of MT1-MMP in atherogenesis have been limited. Schneider et al used a bone marrow transplant system to transfer MT1-MMP–null bone marrow cells into atherogenic *Ldlr*^{−/−} mice to assess the role of the proteinase when expressed by myeloid cells in atherogenesis.¹³ The reconstitution of atherogenic mice with MT1-MMP–null bone marrow cells did not alter the size of the atheroma or the number of infiltrating macrophages but did result in increased collagen content within the atheromatous lesions.¹³ Consequently, although myeloid cell–derived MT1-MMP appears to control collagen turnover, the role of MT1-MMP in regulating atherogenic responses in non–myeloid cell populations remains unknown.

Despite the paucity of information regarding the role of MT1-MMP in atherogenesis, MT1-MMP heterozygous mice, which do not display any of the severe developmental phenotypes observed in the MT1-MMP–null mice, have been reported to display a protected status from both obesity induced by a high fat diet¹⁴ and neointima formation secondary to carotid injury.¹⁵ Given the attenuated responses of MT1-MMP heterozygous animals to pathologic stresses, we initially hypothesized that these mice might likewise be

protected from hypercholesterolemic atherogenesis. Contrary to our expectations, we now report that atherogenesis is significantly enhanced in heterozygous *Mmp14*^{+/-}*Apoe*^{-/-} mice. To determine the cellular mechanisms by which MT1-MMP limits the progression of atherogenesis, we extended our analyses to include newly characterized conditional knockout mice to selectively target MT1-MMP expression in adipose tissue, macrophages, or VSMCs in APOE (apolipoprotein E)–null mice. Unexpectedly, we found that MT1-MMP expressed by VSMCs, and not by either adipocytes or macrophages, exerts a profound protective effect against the progression of proliferative atherosclerotic lesions in *Apoe*^{-/-} mice. Together, these results constitute the first example of MT1-MMP serving as an antiatherogenic enzyme by directly regulating VSMC function and proliferation in the *in vivo* setting.

Material and Methods

Animals

Apoe^{-/-} mice¹⁶ were purchased from the Jackson Laboratory. MT1-MMP heterozygous *Mmp14*^{+/-} mice were maintained on a C57BL6/J background with >5 generations of backcrossing.^{14,17} *Mmp14*^{+/-} mice were crossed to *Apoe*^{-/-} mice to generate *Mmp14*^{+/-}*Apoe*^{+/-} breeders. *Mmp14*^{+/-}*Apoe*^{+/-} mice were used for breeding with *Apoe*^{-/-} mice to generate *Mmp14*^{+/-}*Apoe*^{-/-} mice and their littermate *Mmp14*^{+/+}*Apoe*^{-/-} mice for this study. *Mmp14*^{F/F} mice were generated as described previously.¹⁸ These mice were crossed to *SM22α-Cre* (Tg[Tagln-cre]1Her/J),¹⁹ *Csf1r-Cre*, or *Fabp4-Cre-ERT2* transgenic mice (gift from Pierre Chambon, Institute of Genetics and Molecular and Cellular Biology, France),²⁰ and then further crossed to *Apoe*^{-/-} mice.

Atherosclerosis Study

The atherogenic Western diet, composed of 17% (kcal/kcal) protein, 43% carbohydrate, and 41% fat with 1.5 g/kg cholesterol, was purchased from Research Diets. Male and female mice were fed a Western diet for 12 weeks beginning at 8 weeks of age. All procedures were approved by the University of Michigan committee on the use and care of animals, conforming to the guidelines of the International Association for Assessment and Accreditation of Laboratory Animal Care.

Morphometric Analysis of Atherosclerosis

After euthanasia by CO₂ asphyxiation, blood was collected through portal veins. Animals were perfused with PBS and then 10% formalin in PBS through their left ventricles at a rate

of 1 mL/min, as described previously.²¹ Arterial trees were carefully dissected to include the brachiocephalic, left common carotid, and subclavian arteries, as well as the descending thoracic and abdominal aortas with the bilateral iliac arteries. Adipose tissues attached to the arteries were carefully removed under a dissecting microscope. After Oil Red O staining and repeated washing in ethanol and water, aortic trees were pinned against a black background, and the aortic trees were digitally photographed under a dissecting microscope.²² Oil Red O-positive areas were quantified as the percentage of plaque area per total arterial tree or abdominal aorta.

Collagen Staining and Histologic Analysis

Sections were stained with hematoxylin and eosin and sirius red.²³ The atheroma area and vascular wall area were quantified in cross-sections using ImageJ software (National Institutes of Health), and the average plaque and vascular wall areas were determined. Immunostaining was performed using the ABC system. The primary antibodies used were rabbit polyclonal anti- α -smooth muscle actin (anti- α -SMA) antibody, anti-F4/80 antibody, and anti-Ki67 antibody.

Vascular Smooth Muscle Cells

Mouse aortic smooth muscle cells were isolated with collagenase digestion, as described by others.²⁴ Isolated primary mouse VSMCs were cultured in high-glucose DMEM with 10% FBS and passed twice before experiments. Mouse primary VSMCs immortalized with the SV40 large T antigen were purchased from ATCC.²⁵

3-Dimensional Spheroid Culture

Cells (2×10^4) were cultured as hanging droplets in a 384-well Perfecta3D hanging droplet plate (3D Biomatrix) for 48 hours before assays.²⁶ Cells were cultured in high-glucose DMEM with 10% FBS medium supplemented with 0.24% Methocel A4M (Dow).

Whole-Genome Expression Analysis

The total RNA was extracted from cultured primary VSMCs. Two independent pairs of samples were used for the DNA microarray experiments. Labeled cRNA was hybridized to Affymetrix Mouse Gene ST 2.1 strips at the University of Michigan DNA Sequencing Core. Expression values were calculated using a robust multiarray average. Probe sets that showed >2-fold difference between the groups with a minimal expression value >2⁴ in at least 1 of the samples were chosen for further statistical analyses. Data analysis was performed

with R version 3.1.1, and a heat map was created using the *gplots* package (R package version 2.17.0, <http://CRAN.R-project.org/package=gplots>). Significant biological pathways represented by the differentially expressed genes were determined using PANTHER (<http://pantherdb.org/>).

Statistical Analyses

Values were expressed as mean \pm SEM. The distribution of weight, fat mass, cholesterol profile, fasting insulin, and glucose levels between 2 groups were analyzed using a 2-tailed, unpaired Student *t* test. To assess the differences in atherogenesis between the multiple groups, 2-way ANOVA was used, followed by a post hoc pairwise comparison using the Tukey procedure. *P* values <0.05 were considered significant.

Results

The Effect of the MT1-MMP Gene Dose on Fat Mass and Dyslipidemia in APOE-Null Mice

We previously demonstrated that MT1-MMP heterozygosity renders mice resistant to obesity induced by a high fat diet.¹⁴ Based on this finding, we hypothesized that the allelic reduction of the MT1-MMP gene would protect mice from hypercholesterolemic atherosclerosis, a disease process that is often associated with obesity in humans.²⁷ As such, we crossbred MT1-MMP heterozygous (*Mmp14*^{+/-}) mice with APOE-null mice to generate *Mmp14*^{+/-}*ApoE*^{-/-} mice and examined the effects of MT1-MMP heterozygosity on weight, fat mass, blood glucose, and insulin levels as well as cholesterol profiles. As expected, heterozygous (HT) *Mmp14*^{+/-}*ApoE*^{-/-} male mice on a Western diet were leaner than littermate wild-type (WT) *Mmp14*^{+/+}*ApoE*^{-/-} mice (WT 33.0 \pm 1.0 g, HT 29.0 \pm 0.9 g, *n*=9 each, *P*=0.009; Figure 1A). When fat mass was assessed at the end of the 12-week Western diet, the total and epididymal fat masses were significantly smaller in the *Mmp14*^{+/-}*ApoE*^{-/-} than *Mmp14*^{+/+}*ApoE*^{-/-} male mice (percentage of total fat mass per weight: WT 5.1 \pm 0.3%, HT 3.6 \pm 0.6%, *n*=9 each, *P*=0.03; percentage of epididymal fat per weight: WT 3.4 \pm 0.2%, HT 2.2 \pm 0.3%, *n*=9 each, *P*=0.007; Figure 1B). Fasting blood glucose levels were similar between the groups (WT 162 \pm 43 [n=8] versus HT 161 \pm 27 mg/dL [n=9], *P*=0.5); however, the fasting insulin concentration was substantially lower in the MT1-MMP heterozygous mice (WT 11.8 \pm 4.3 [n=8] versus HT 3.8 \pm 0.6 mU/L [n=9], *P*=0.04), suggesting an increased insulin sensitivity of *Mmp14*^{+/-}*ApoE*^{-/-} mice that occurs in parallel with their leaner phenotype. Of note, MT1-MMP heterozygosity did not change the blood cholesterol levels in APOE-null mice fed a Western diet (total cholesterol: WT

1021±59 [n=8] versus HT 1012±52 mg/dL [n=9], $P=0.9$; direct low-density lipoprotein: WT 359±27 versus HT 349±23 mg/dL, $P=0.8$; Figure 1C). Consistent with their leaner phenotype and relative insulin sensitivity, the blood triglyceride content tended to be lower in HT mice, but this difference did not reach statistical significance (WT 142±10 mg/dL [n=8], HT 118±11 mg/dL [n=9], $P=0.1$).

Whole-Body MT1-MMP Heterozygosity Accelerates Atherogenesis

MT1-MMP WT and HT mice were fed a Western diet for 12 weeks beginning at 8 weeks of age. Contrary to our

prediction, atherogenesis was more advanced in $Mmp14^{+/-}Apoe^{-/-}$ mice compared with $Mmp14^{+/+}Apoe^{-/-}$ littermate controls (Figure 1D). Particularly, advanced atherogenesis was notable in the abdominal aorta and iliac/femoral arteries of $Mmp14^{+/-}Apoe^{-/-}$ mice (Figure 1D arrows). The percentage of total plaque area was increased by 21% in male mice ($Mmp14^{+/+}Apoe^{-/-}$ 14.9±0.9% versus $Mmp14^{+/-}Apoe^{-/-}$ 18.1±0.8%, n=7 each, $P=0.04$; Figure 1E, left), whereas the abdominal percentage of plaque area was increased by 200% (2.3±0.5% versus 6.9±0.5%, n=7 each, $P<0.0001$; Figure 1E, right). In female mice, the total plaque area in $Mmp14^{+/-}Apoe^{-/-}$ animals was increased by 56% (15.1±1.3% [n=4] versus 23.6±1.6% [n=10], $P=0.002$; Figure 1F, left), with the

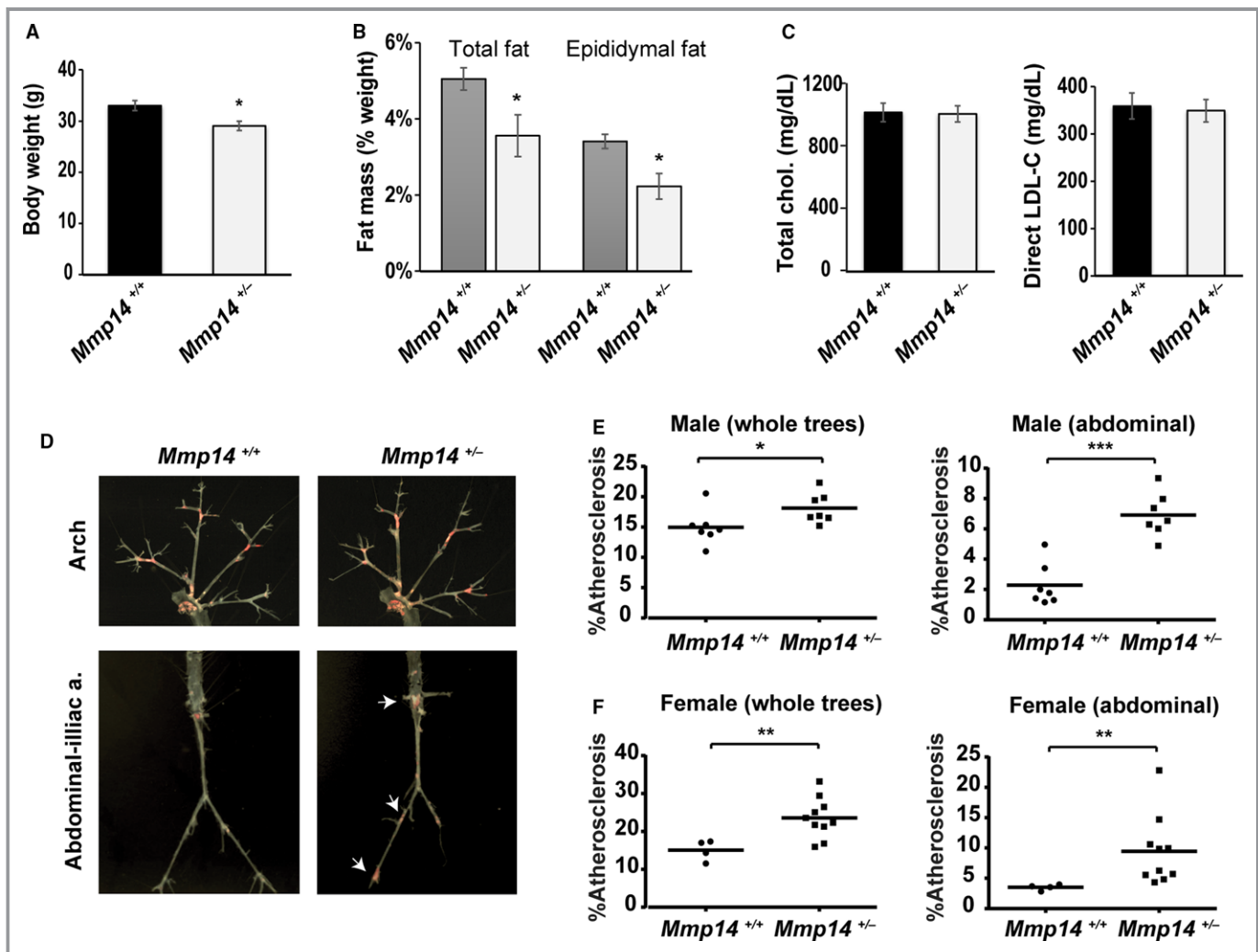


Figure 1. MT1-MMP (membrane-type 1 matrix metalloproteinase) heterozygosity promotes atherosclerosis. A, $Mmp14^{+/+}Apoe^{-/-}$ mice and $Mmp14^{+/-}Apoe^{-/-}$ mice were fed a Western diet for 12 weeks beginning at 8 weeks of age. Body weight (g) at the end of study. B, Percentage of fat mass (wt/wt) of total (epididymal plus inguinal) and epididymal fat pads. C, Fasting serum cholesterol (total and direct low-density lipoprotein) levels. Mean±SEM, n=8 and n=10, respectively; * $P<0.05$. D, Atherosclerotic lesions detected with Oil Red O staining in $Mmp14^{+/+}Apoe^{-/-}$ and $Mmp14^{+/-}Apoe^{-/-}$ male mice. Arrows point to the increased atherosclerosis distributed in abdominal aorta and iliac arteries specifically, as found in $Mmp14^{+/-}Apoe^{-/-}$ mice. E and F, Oil Red O-positive atherosclerotic plaque areas quantified in all aortic trees and abdominal aortas in male mice (n=7 each) and female mice (n=4 and n=10). Mean±SEM, * $P<0.05$, ** $P<0.005$, *** $P<0.0005$. a. indicates artery.

abdominal plaque area increasing by 171% relative to the *Mmp14*^{+/+}*ApoE*^{-/-} female controls ($3.5 \pm 0.2\%$ [n=4] versus $9.5 \pm 1.8\%$ [n=10], $P=0.002$; Figure 1F, right).

We next examined left carotid artery sections to assess the structure of the atherosclerotic plaque and the associated level of vascular wall remodeling. Interestingly, the average plaque area of the *Mmp14*^{+/-}*ApoE*^{-/-} mice was 3 times as large as that of the *Mmp14*^{+/+}*ApoE*^{-/-} mice, but this was not statistically significant given the variable severity of atherosclerosis in the heterozygous group (WT $59 \pm 7 \times 10^3 \mu\text{m}^2$ versus HT $189 \pm 84 \times 10^3 \mu\text{m}^2$, n=6 each, $P=0.15$; Figure 2A). Concurrent with a trend of increased atherosclerosis, we observed a 1.7-fold increase in the

vascular wall area, underscoring the presence of outward vascular wall remodeling in MT1-MMP heterozygous APOE-null mice ($133 \pm 16 \times 10^3 \mu\text{m}^2$ versus $234 \pm 19 \times 10^3 \mu\text{m}^2$, n=6 each, $P=0.004$). Furthermore, both the atherosclerotic plaques and the vascular walls of MT1-MMP HT mice displayed an increased collagen fiber content relative to WT mice, as assessed by sirius red staining (sirius red-positive area: WT $26.6 \pm 3.3\%$ versus HT $44.0 \pm 4.7\%$, n=6 each, $P=0.009$; Figure 2B), suggesting that MT1-MMP heterozygosity promoted vascular wall arteriosclerosis along with plaque formation in the APOE-null background. MT1-MMP HT mice also displayed an apparent loss of a contractile phenotype (ie, loss of SMA staining) coupled with disrupted elastic lamina,

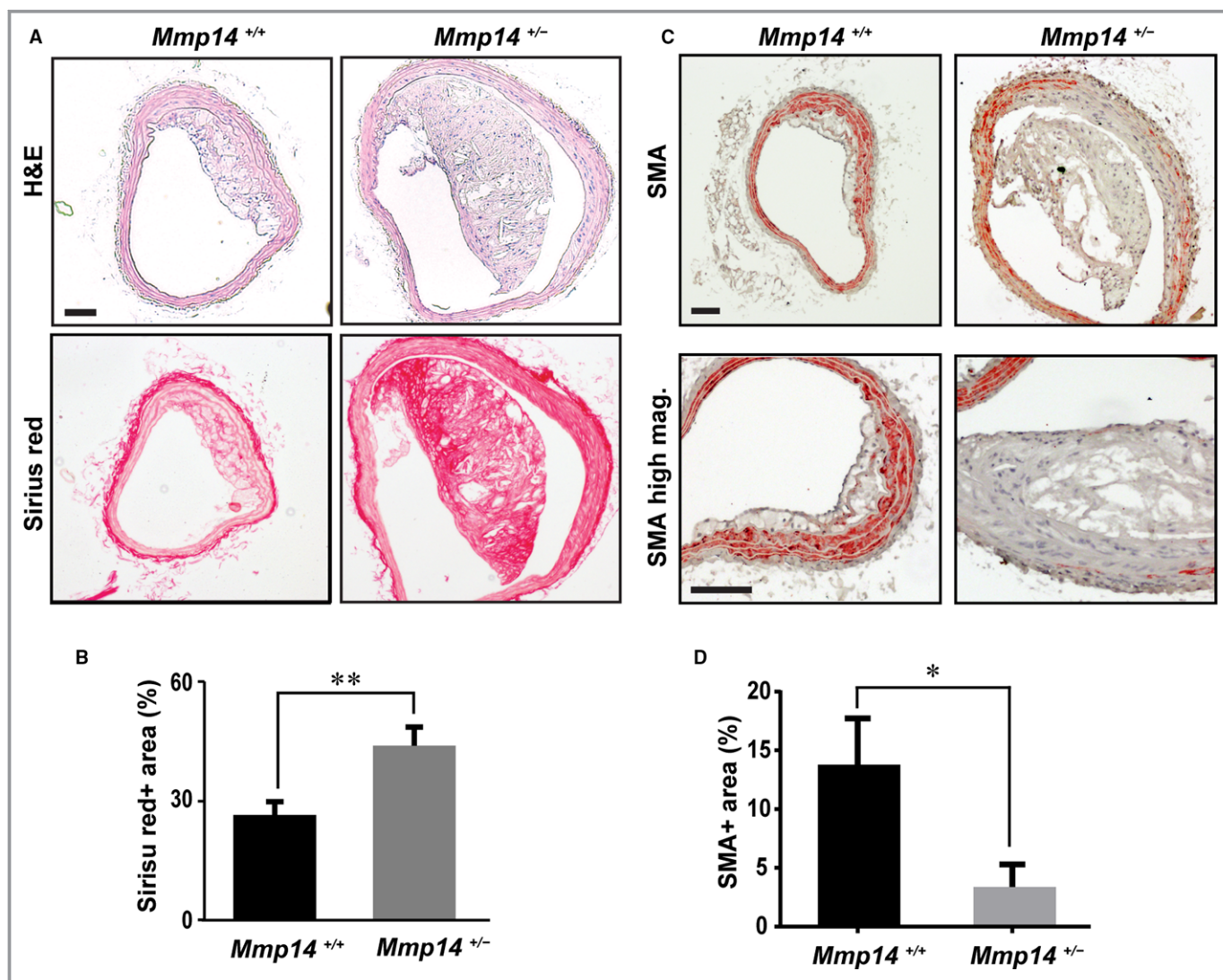


Figure 2. MT1-MMP (membrane-type 1 matrix metalloproteinase) heterozygosity promotes plaque formation and outward vascular remodeling. A, Representative histology sections of left common carotid arteries. Hematoxylin and eosin (H&E) and sirius red staining. Scale=100 μm . B, Sirius red-positive area (%). C, Immunostaining of smooth muscle actin (SMA) in vascular walls and atherosclerotic plaques (orange). Nuclei were counterstained (blue). Lower panels are of higher magnification. Scale=100 μm . D, SMA-positive area (percentage). Mag indicates magnification. * $P<0.05$, ** $P<0.005$

which in turn elicited more complex and advanced atherosclerotic lesions (Figure 2C and 2D).

MT1-MMP Gene Targeting in VSMCs Accelerates Atherosclerosis Progression

Although MT1-MMP heterozygosity was found to promote atherogenesis, the cellular mechanisms underlying the aggravated atherogenesis were unclear. In obesity, perivascular adipose tissues play a key role in atherogenesis.²⁸ In contrast, dysfunctional VSMCs might also be responsible for inducing

inflammatory atherogenesis.⁴ Because MT1-MMP is highly expressed in both adipocytes^{9,10} and VSMCs,¹⁵ we sought to use tissue-specific knockout mice in an effort to determine the cell type responsible for the MT1-MMP-dependent regulation of atherogenesis. When male mice in each group were fed a Western diet, we observed markedly augmented atherogenesis and aneurysm formation only with VSMC-specific MT1-MMP gene targeting (ie, *SM22 α -Cre*[+]*Mmp14*^{F/F}*Apoe*^{-/-} mice), but not following adipocyte MT1-MMP gene targeting (ie, *aP2-Cre-ERT2*[+]*Mmp14*^{F/F}*Apoe*^{-/-} mice; Figure 3A). Atherogenesis in *SM22 α -Cre*(+)*Mmp14*^{F/F}*Apoe*^{-/-}

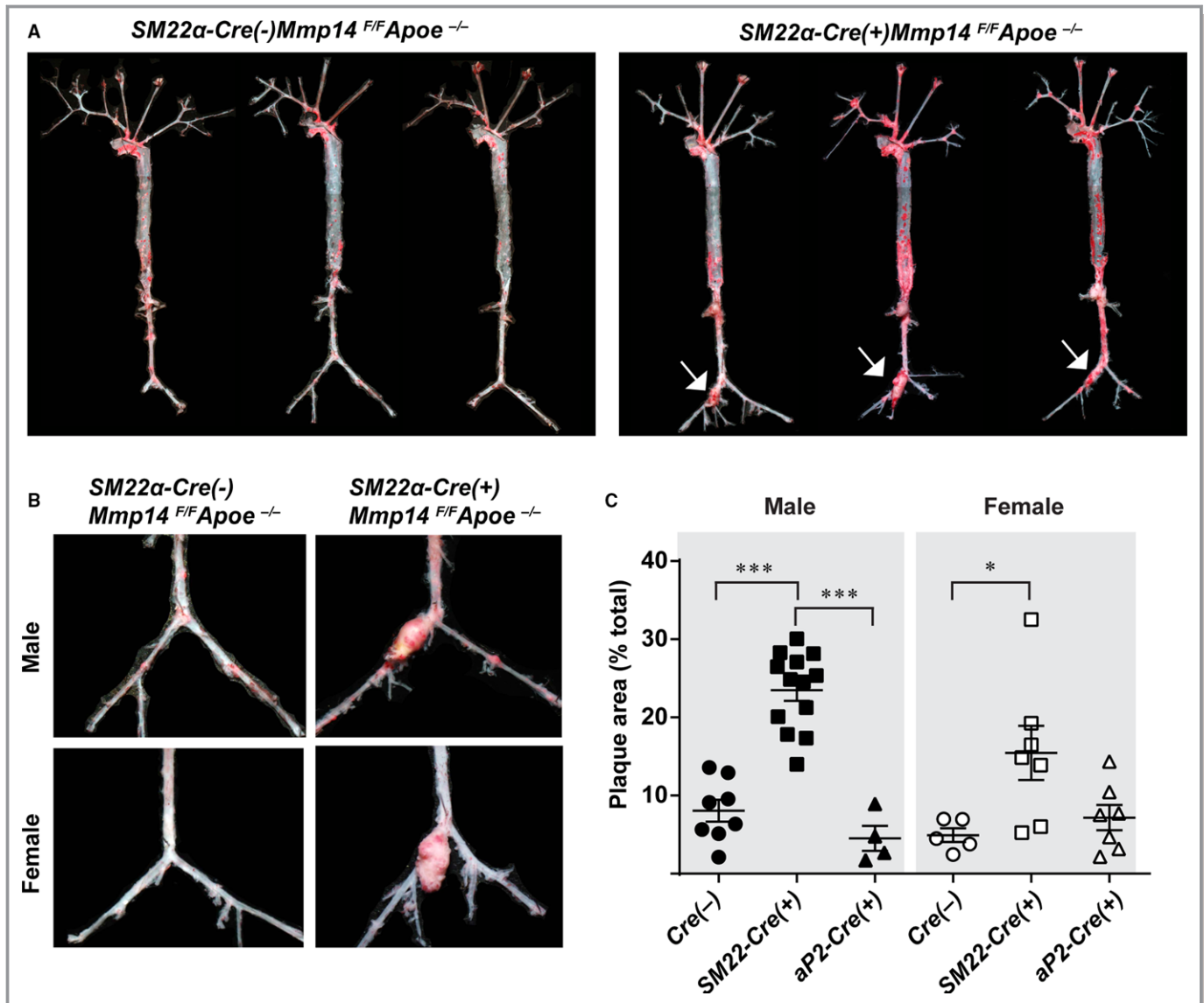


Figure 3. Vascular smooth muscle cell MT1-MMP (membrane-type 1 matrix metalloproteinase) gene targeting promotes atherosclerosis and aneurysm formation. A, Whole arterial trees assessed for Oil Red O–positive atherosclerotic plaque area (red). Arrows point to atherosclerotic aneurysms. Representative arterial trees from *SM22 α -Cre(-)Mmp14*^{F/F}*Apoe*^{-/-} and *SM22 α -Cre(+)-Mmp14*^{F/F}*Apoe*^{-/-} mice are shown; n=13 and n=20, respectively. B, Higher magnification of aortic aneurysms found in *SM22 α -Cre(+)-Mmp14*^{F/F}*Apoe*^{-/-} mice. C, Percentage of plaque area in *Cre(-)Mmp14*^{F/F}*Apoe*^{-/-}, *SM22 α -Cre(+)-Mmp14*^{F/F}*Apoe*^{-/-}, *aP2-Cre-ERT2(+)-Mmp14*^{F/F}*Apoe*^{-/-} mice, males and females (n=8, n=13, and n=4 in male mice, and n=5, n=7, and n=7 in female mice, respectively). **P*<0.05, ****P*<0.0005.

mice frequently extended to femoral arteries with significant outward remodeling having been noted, in tandem with aneurysm formation in the iliac arteries (Figure 3A and 3B). Importantly, total plaque area was increased by 190% in *SM22 α -Cre(+)**Mmp14^{F/F}Apoe^{-/-}* male mice compared with *Cre(-)**Mmp14^{F/F}Apoe^{-/-}* male mice ($8.0 \pm 1.4\%$ [$n=8$] versus $23.5 \pm 1.4\%$ [$n=13$], $P<0.0001$) and 210% in female mice ($4.9 \pm 0.9\%$ [$n=5$] versus $15.5 \pm 3.5\%$ [$n=7$], $P=0.03$). In contrast, significant differences were not observed between Cre-negative controls and the adipose-specific MT1-MMP deletion model (Figure 3C and Figure S1), suggesting that the VSMCs are the primary cell type that mediates MT1-MMP-dependent modulation of atherogenesis progression.

The Loss of VSMC MT1-MMP Leads to Proliferative Atherosclerotic Lesions and Aneurysm Formation

After 12-week Western diet feeding, *SM22 α -Cre(+)**Mmp14^{F/F}Apoe^{-/-}* mice developed extensive atherosclerosis in their common iliac arteries followed by aneurysm formation (Figure 4A and 4B). No aneurysm formation was observed in the *Cre(-)**Mmp14^{F/F}Apoe^{-/-}* mice (8 male and 5 female mice), whereas 11 of 12 male and 6 of 7 female *SM22 α -Cre(+)**Mmp14^{F/F}Apoe^{-/-}* mice developed strikingly enlarged aneurysms that were readily observable on dissection (Figure 3B). These dysmorphic lesions displayed significant vascular wall thickening as well as atheroma formation (Figure 4A). Masson's Trichrome and Verhoeff–Van Gieson staining demonstrated the disruption and loss of elastic laminae (Figure 4A). SMA staining showed an increased number of SMA⁺ cells in vascular walls as well as within atheroma, where Ki67 staining confirmed that large numbers of SMA⁺ cells existed in a proliferative state (Figure 4A and 4D). Infiltration of F4/80-positive cells was observed in the atheroma and the vascular walls of affected vessels (Figure 4A, F4/80 staining) but to a lesser extent compared with VSMCs. Image quantification of the lesions confirmed an increased atheroma area (Figure 4B) and outward remodeling (Figure 4C), which were coupled with an increased number of proliferating VSMCs (Figure 4D). Because macrophages are potentially targeted by SM22 α promoter-driven Cre expression,²⁹ we specifically targeted these cells using *Csf1r-Cre(+)**Mmp14^{F/F}Apoe^{-/-}* mice and examined atherosclerosis and aneurysm formation. Neither littermate control *Csf1r-Cre(-)**Mmp14^{F/F}Apoe^{-/-}* mice nor *Csf1r-Cre(+)**Mmp14^{F/F}Apoe^{-/-}* mice developed atherosclerotic iliac aneurysm after 12 weeks of Western diet ($n=7$ for each group tested), and no significant differences in the sizes of atherosclerosis lesions were observed ($n=4$ each).

Proinflammatory and Metabolically Dysfunctional MT1-MMP-Null VSMCs

To assess the role of MT1-MMP in VSMC function, we isolated primary VSMCs from descending aortas. As expected, VSMCs isolated from *SM22-Cre(+)**Mmp14^{F/F}Apoe^{-/-}* mice demonstrated specific Cre expression along with the suppression of MT1-MMP gene expression (Figure S2). In vitro, MT1-MMP-null VSMCs displayed a flattened, spread shape with higher stress fiber formation (Figure 5A), whereas the expression of other MMPs (eg, MMP-2, MMP-8, MMP-9, MMP-13, and MT2-MMP [MMP15]), were not significantly different between control and MT1-MMP-deleted cells (Figure S2). The *Acta2* gene, which encodes α -SMA, was expressed equally in primary VSMCs isolated from *SM22-Cre(-)**Mmp14^{F/F}Apoe^{-/-}* and *SM22-Cre(+)**Mmp14^{F/F}Apoe^{-/-}* mice (Figure S2). To gain further insight into the effects of MT1-MMP gene targeting in VSMCs, whole-genome transcriptome analysis was performed. Using a minimum 2-fold difference as a cutoff, 414 genes were found to be differentially expressed between the 2 groups (the top 70 genes are shown in Figure 5B, and all differentially expressed genes are listed in Table S1; the microarray data is available at NCBI Gene Expression Omnibus [GSE] as GSE100661). Interestingly, the genes upregulated in *SM22 α -Cre(+)**Mmp14^{F/F}Apoe^{-/-}* VSMCs (>2.3-fold change) were aggregated in the pathways of inflammation and cell killing (Figure 5C), suggesting the acquisition of a proinflammatory phenotype in MT1-MMP-null VSMCs.

MT1-MMP Gene Targeting Promotes VSMC Proliferation in 3-Dimensional Cell–Cell and Cell–ECM Contexts

To gain insights into the mechanism by which MT1-MMP-null VSMCs engage in the formation of proliferative atherosclerotic lesions, we developed an in vivo-like 3-dimensional (3-D) spheroid culture system in which in vivo-like cell–cell and cell–ECM interactions could be recapitulated. Using Ki67 as an index of proliferative responses, MT1-MMP-null primary VSMCs displayed markedly higher activity relative to WT cells (Figure 6A and 6B). To determine whether the observed differences in cell proliferation were a direct consequence of MT1-MMP gene targeting (ie, as opposed to a secondary response of VSMCs recovered from the advanced atherogenic lesions found in VSMC-knockout mice), we used immortalized mouse primary VSMCs to further define the role of MT1-MMP in regulating VSMC proliferation. In 3-D spheroid culture, similar to the findings obtained with freshly isolated VSMCs, small interfering RNA-mediated MT1-MMP gene silencing in mouse VSMCs induced a marked increase in the number of Ki67-positive VSMCs (Figure 6C and 6D). Of note, under 2-D culture

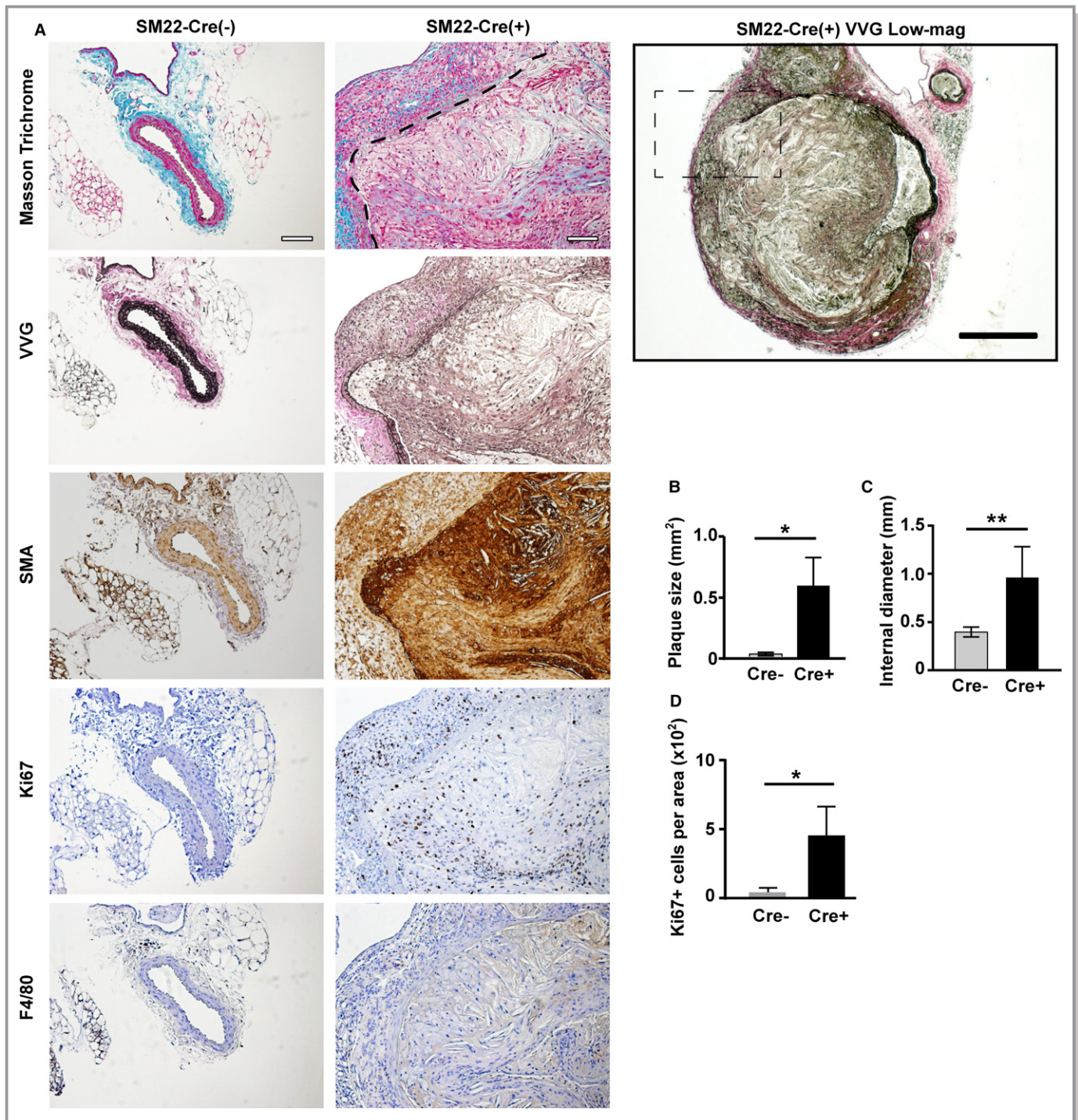


Figure 4. The loss of vascular wall integrity and vascular smooth muscle cell (VSMC) proliferation in VSMC MT1-MMP (membrane-type 1 matrix metalloproteinase) knockout mice. A, Atherosclerotic aneurysms found in iliac arteries of *SM22α-Cre(+)/MMP14^{F/F}ApoE^{-/-}* mice. Masson’s Trichrome staining; the border between the vascular wall and the atheroma is demarcated with a dashed line. Verhoeff–Van Gieson staining (VVG), smooth muscle actin (SMA) staining, Ki67 staining, and F4/80 (a macrophage marker) staining. Scale=100 μm. The lower magnification (×4) micrograph of *SM22α-Cre(+)/MMP14^{F/F}ApoE^{-/-}* VVG staining on the right. Scale=200 μm. The lesion in the dashed square is shown on the left. B, Plaque area. C, The internal diameter of iliac arteries. D, Ki67-positive area. Mean±SEM; n=5 and n=7 for each group. One-way ANOVA. **P*<0.05, ***P*<0.005.

conditions, MT1-MMP silencing exerted minimal effects on mouse VSMC proliferation (Figure 6E and 6F). Taken together, these results support a model in which MT1-

MMP plays a required role in regulating VSMC proliferative activity but only under 3-D conditions that more closely recapitulate the in vivo environment.

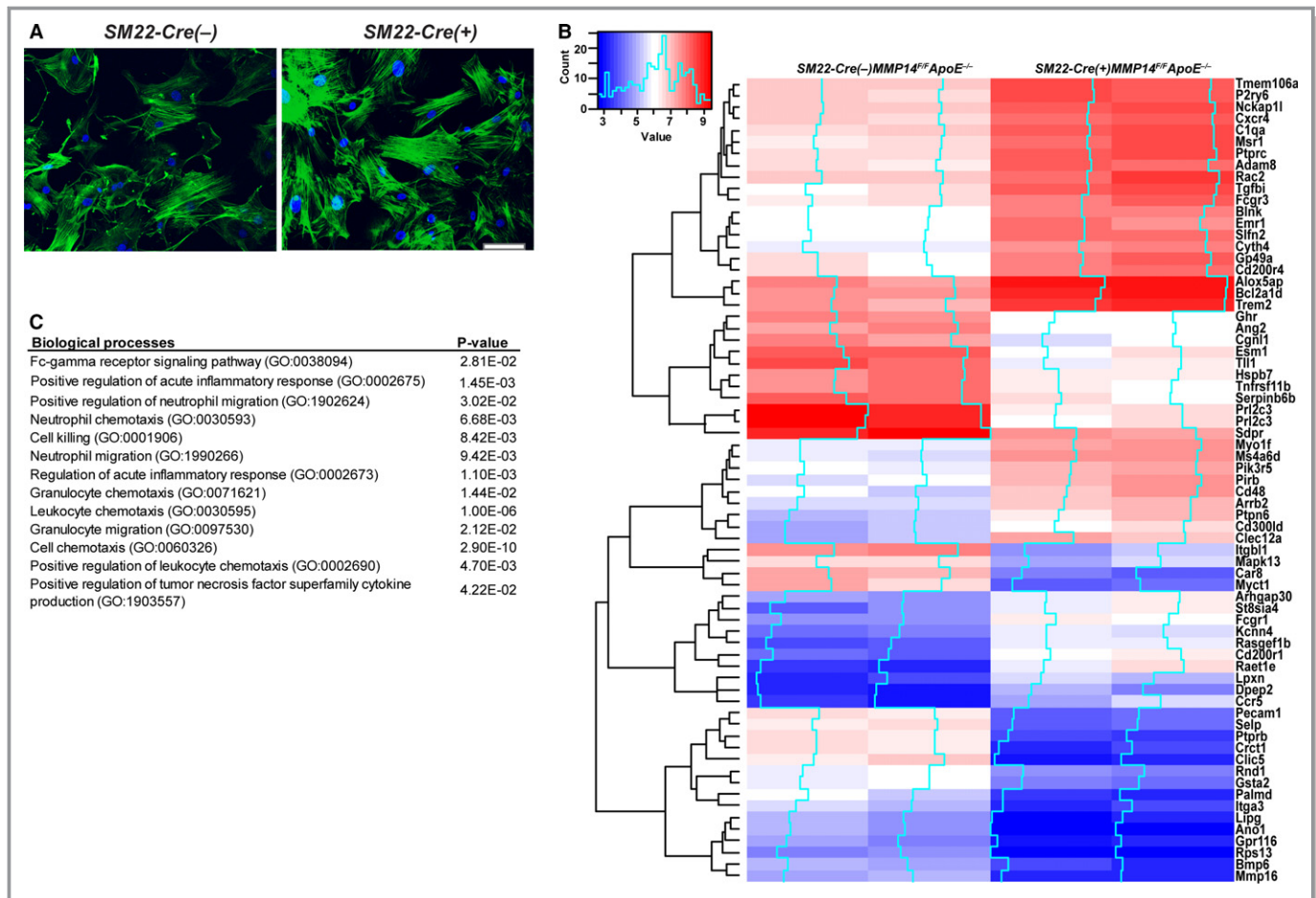


Figure 5. Proinflammatory gene expression in MT1-MMP (membrane-type 1 matrix metalloproteinase)-null vascular smooth muscle cells (VSMCs). A, Primary aortic VSMCs isolated from *Cre(-)Mmp14^{F/F}ApoE^{-/-}* and *SM22α-Cre(+)/Mmp14^{F/F}ApoE^{-/-}* mice. F-actin (green), nuclei (blue). B, Representative genes differentially expressed in VSMCs from 2 independent pairs of *Cre(-)Mmp14^{F/F}ApoE^{-/-}* and *SM22α-Cre(+)/Mmp14^{F/F}ApoE^{-/-}* mice. C, Gene Ontology (GO) biological processes represented by the genes upregulated in VSMCs isolated from the *SM22α-Cre(+)/Mmp14^{F/F}ApoE^{-/-}* mice.

Discussion

MMP family members play a key role in ECM turnover in a wide variety of developmental and disease processes.³⁰ Among the collagen-degrading MMPs, secreted (MMP-3, MMP-8, MMP-13) and membrane-type MMPs (MT1- and MT2-MMP) display distinct temporospatial differences in their patterns of expression and activity.⁹ Unlike other MMPs, MT1-MMP (MMP14) is the only family member whose activity is indispensable for postnatal development.^{10,11} Because of the premature morbidity and mortality displayed by MT1-MMP-null mice, the role of the proteinase in cardiovascular disease has remained elusive. To date, the only MT1-MMP-expressing cellular compartment tested in a mouse atherogenesis model was bone marrow-derived myeloid cells; however, no substantial impact on atheroma size was observed following bone marrow reconstitution with *Mmp14^{-/-}* cells.¹³ In our study, we identified the critical role played by VSMC-derived MT1-

MMP in regulating the progression of atherosclerotic lesions and the associated formation of vascular aneurysms.

Previously, we demonstrated that MT1-MMP heterozygosity protects C57BL/6 mice from diet-induced adipose tissue expansion.¹⁴ Similarly, in this study, heterozygous *Mmp14^{+/-}* mice displayed a leaner phenotype relative to *Mmp14^{+/+}* mice in an APOE-null background. Consistent with their leaner phenotype, MT1-MMP heterozygous mice displayed higher insulin sensitivity than WT mice. Given the metabolically improved status of *Mmp14^{+/-}* mice, we initially hypothesized that MT1-MMP heterozygosity would protect mice from hypercholesterolemic atherosclerosis, which is often associated with increased adiposity. Contrary to our expectations, MT1-MMP heterozygous APOE-null mice developed more extensive atherosclerotic lesions than MT1-MMP-sufficient APOE-null mice, suggesting a potentially beneficial role for MT1-MMP in limiting disease progression. The results also

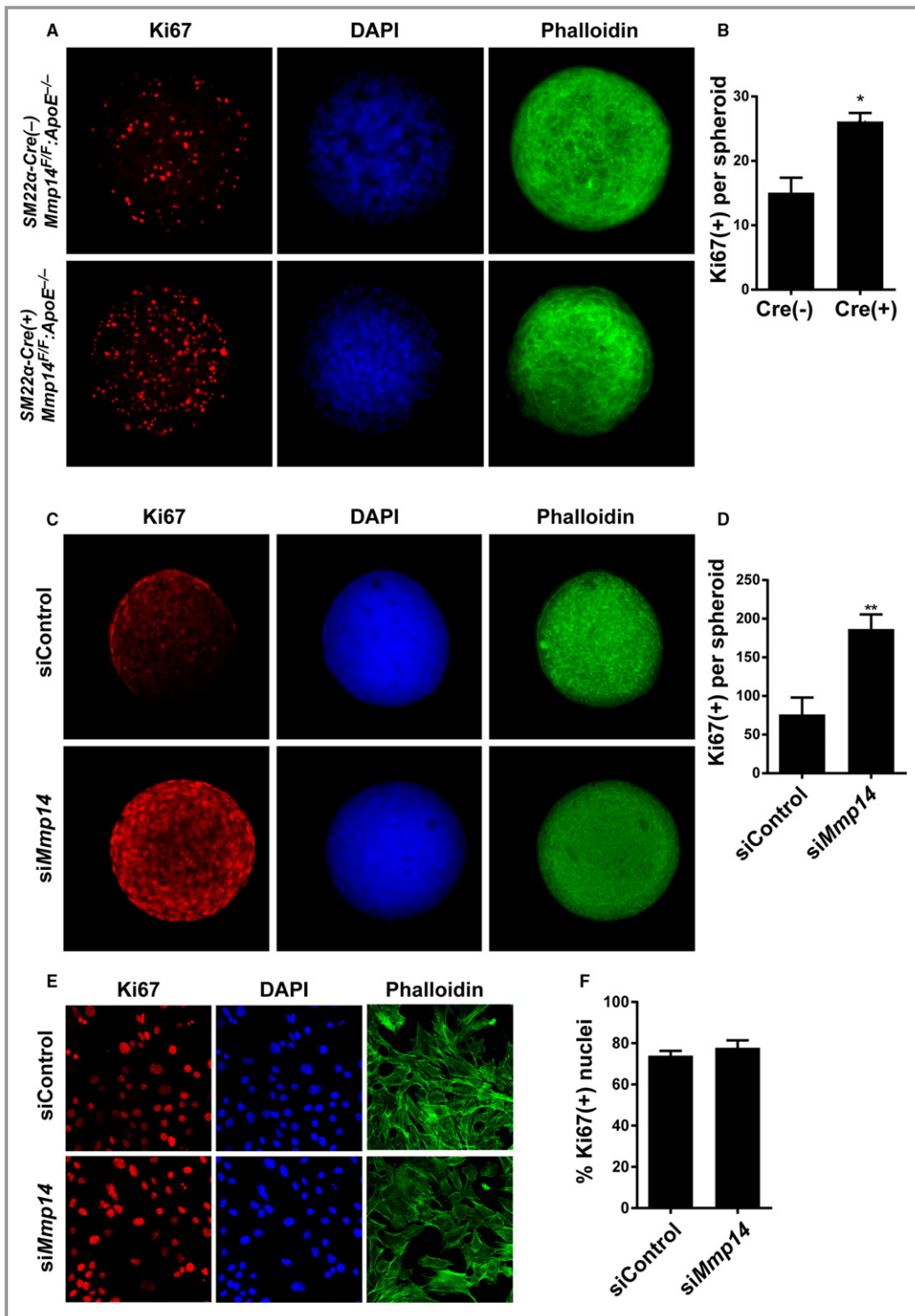


Figure 6. MT1-MMP (membrane-type 1 matrix metalloproteinase) limits vascular smooth muscle cell (VSMC) proliferation in 3-dimensional (3-D) organoids. A, Primary VSMCs isolated from *Cre(-)* *Mmp14^{F/F} ApoE^{-/-}* mice and *Cre(+)* *Mmp14^{F/F} ApoE^{-/-}* mice were cultured as a 3-D spheroids for 48 hours and stained for Ki67 (red), nuclei (DAPI, blue), and actin (phalloidin, green). B, Quantified intensity of Ki67 staining per spheroid. n=5 to 7. **P*<0.05. C, Immortalized mouse VSMCs (MOVAS) transiently transfected with small interfering RNA (siRNA) control (siControl) and MT1-MMP siRNA (siMmp14). Ki67 (red), nuclei (blue), actin (green). D, Ki67 staining intensity per spheroid of MOVAS. ***P*<0.005. E, 2-D cultured MOVAS transfected with control and MT1-MMP siRNA. Ki67 (red), nucleus (blue), and actin (green). F, Ki67-positive nuclei per total nuclei count.

suggest that the inverse relationship observed between fat mass and atherosclerosis—the so-called obesity paradox in humans—may reflect the independent biological effects exerted by a cohort of modifier genes, including MT1-MMP, on adipose tissue and vascular function.

To define the cellular mechanisms by which MT1-MMP exerts its antiatherogenic effects, we embarked on a series of studies aimed at tissue-specific MT1-MMP gene targeting in APOE-null mice. In the early stages of our efforts, we focused on 2 cell types: adipocytes and VSMCs. We initially hypothesized that the loss of adipocyte MT1-MMP would modify atherogenesis via the potentially causal links that exist between adipose tissue and the vascular wall.³¹ In APOE-null mice, however, we were unable to observe a significant impact on atherogenesis following gene targeting of adipocyte-derived MT1-MMP. In contrast, the SM22 α -Cre-mediated loss of VSMC MT1-MMP strikingly aggravated atherosclerosis progression in APOE-null mice. Whole-genome transcriptome analyses indicated that a series of proinflammatory genes were upregulated in MT1-MMP-null VSMCs, a finding consistent with the proatherogenic phenotype of SM22 α -Cre(+) Mmp14^{F/F}Apoe^{-/-} mice. Furthermore, our in vitro studies demonstrated that MT1-MMP targeting in either primary or immortalized VSMCs promotes cell proliferation under 3-D spheroid culture conditions.²⁶ As such, 3-D spheroid culture appears to reflect a set of conditions that better reflect our in vivo findings and, as such, can be used to more faithfully address cellular behavior in tissue-like contexts by re-creating cell–cell and cell–ECM interactions ex vivo. Indeed, previous work has demonstrated that VSMC proliferative activity can be regulated by cell–cell adhesion^{32–34} and cell–ECM interactions.^{35,36} Of note, the enhanced proliferative responses displayed by MT1-MMP-null VSMCs were not observed under conventional 2-D culture conditions in which the cell–cell and cell–ECM interactions that are encountered in vivo are replaced by cell culture atop a nonphysiologic, planar, and rigid substratum. Finally, it is interesting to note that the proliferative effects of MT1-MMP gene silencing were not observed in other cell types, for example, 3T3-L1 preadipocytes (data not shown), reinforcing the unique role played by MT1-MMP in VSMC biology.

In considering the mechanisms by which MT1-MMP might control proliferative activity, efforts are complicated by the proteinase's broad substrate repertoire, ranging from type I collagen³⁷ to CD44³⁸ and cadherins.³⁹ As such, MT1-MMP can potentially regulate VSMC proliferation by degrading any number of membrane-associated protein targets as well as pericellular ECM molecules, thereby modifying both cell–cell adhesion and cell–ECM interaction. In atherosclerosis, the expression of adhesion molecules and ECM proteins is highly upregulated⁴⁰; as such, a decrease in MT1-MMP activity would be predicted to trigger the excess accumulation of ECM

macromolecules as well as cell-surface adhesion molecules. At this juncture, we posit that changes in the dynamics of ECM turnover and cell-surface molecule expression occurring within the vascular wall lead to the unregulated proliferation of VSMCs and the development of a proinflammatory phenotype. Interestingly, at least in terms of proliferative responses, the use of a 3-D spheroid model allowed us to recapitulate the MT1-MMP-dependent biological processes ex vivo. Nevertheless, it remains unclear how the cleavage of MT1-MMP substrate(s) accelerates VSMC proliferation in APOE-null mice. This caveat notwithstanding, our data clearly highlight the role played by VSMC-derived MT1-MMP in limiting the progression of proliferative atherosclerotic lesions. Because MT1-MMP is a membrane-bound proteinase, the physical proximity of substrates with the enzyme is likely critical for the protective effects exerted by VSMCs in limiting the expansion of atherosclerotic lesions. Our study also suggests that other atherosclerosis-associated MMPs (eg, MMP-2, MMP-8, MMP-13) do not compensate for the genetic loss of MT1-MMP and are unable to limit atherosclerosis progression. Although MT2-MMP (MMP15) was also expressed in mouse VSMCs (Figure S2), as reported previously in rat VSMCs,⁴¹ the biological phenotypes conferred by MT1-MMP gene loss were not rescued by the presence of MT2-MMP. Differences in the hemopexin domain structure, posttranslational modification, or protein trafficking may underlie the specific effects mediated by MT1-MMP versus MT2-MMP.⁴²

Although increased collagen content within atheroma might be predicted to play a protective role against plaque rupture, collagen accumulation in arterial walls could also accentuate vascular sclerosis and stiffening. In turn, stiff and sclerotic blood vessels could increase luminal shear stress, thereby increasing the chance of plaque rupture. In future studies, an assessment of hemodynamic changes and plaque instability in our model will be required to more accurately define the role of MT1-MMP in cardiovascular disease. Interestingly, in APOE-null mice, arterial wall stiffness is known to be increased through VSMC lysyl oxidase activity.⁴³ In turn, increased tissue stiffness could control VSMC proliferation through the activation of a mechanotransduction pathway, for example, YAP/TAZ transcription activity.⁴⁴ As such, we posit that the pathologic accumulation of ECM macromolecules secondary to the loss of MT1-MMP activity may further promote vascular wall rigidity in the APOE-null mice, leading to hyperproliferative vascular lesions and aneurysm formation. Given that we observed severe atherosclerosis and aneurysm formation in iliac and femoral arteries, site-specific increases in vascular wall thickening and arteriosclerosis are likely related to the distinct mechanical properties of vessel walls observed along the arterial tree.⁴⁵ Indeed, femoral arteries as well as the abdominal aorta are known to display higher wall thickness with lower content of

elastic lamina compared with carotid arteries and thoracic aortas.⁴⁵ Together, differences in mechanical stress and ECM composition may render VSMCs in abdominal aortae and femoral arteries more vulnerable to atherogenic proliferation.

Finally, it remains to be determined whether the inflammatory gene expression profile observed in MT1-MMP-null VSMCs is restricted to atherogenic milieu encountered in vivo. Interestingly, in our hands, the increase in inflammatory gene expression of MT1-MMP-null VSMCs was coupled with decreased mitochondrial activity (T. Akama, PhD, unpublished data, 2016). Furthermore, recent studies have demonstrated a critical role played by a VSMC phenotypic switch to macrophage-like cells in atherogenesis.^{4,46} Because MT1-MMP also regulates inflammatory responses in macrophages,⁴⁷ the proteinase may well play a key role in controlling a complex set of metabolic and phenotypic switching programs that are engaged in atherogenic VSMCs. Although further work is needed to delineate MT1-MMP function during atherogenesis, our work highlights the previously unsuspected vessel wall-protective effects exerted by this membrane-anchored metalloproteinase in the VSMC compartment.

Acknowledgments

We like to thank Dr Pierre Chambon (Institute of Genetics and Molecular and Cellular Biology, France) for sharing *Fabp4-Cre-ERT2* transgenic mice. Current affiliation of Öhman is Duke-Nus Medical School, Singapore.

Sources of Funding

Funding was provided by the McKay Research Grant from University of Michigan Cardiovascular Center, NIH R21HL106332, and R01DK102656 to Chun. NIH R01AI105068-01 to Weiss. NIH Cancer Biology Training Program Grant T32-CA009676 supported Bahr.

Disclosures

None.

References

- Olivetti G, Anversa P, Melissari M, Loud AV. Morphometric study of early postnatal development of the thoracic aorta in the rat. *Circ Res*. 1980;47:417–424.
- Wagenseil JE, Mecham RP. Vascular extracellular matrix and arterial mechanics. *Physiol Rev*. 2009;89:957–989.
- Owens GK, Kumar MS, Wamhoff BR. Molecular regulation of vascular smooth muscle cell differentiation in development and disease. *Physiol Rev*. 2004;84:767–801.
- Bennett MR, Sinha S, Owens GK. Vascular smooth muscle cells in atherosclerosis. *Circ Res*. 2016;118:692–702.
- Page-McCaw A, Ewald AJ, Werb Z. Matrix metalloproteinases and the regulation of tissue remodelling. *Nat Rev Mol Cell Biol*. 2007;8:221–233.
- Kuzuya M, Nakamura K, Sasaki T, Wu Cheng X, Itoharu S, Iguchi A. Effect of MMP-2 deficiency on atherosclerotic lesion formation in apoE-deficient mice. *Arterioscler Thromb Vasc Biol*. 2006;26:1120–1125.
- Laxton RC, Hu Y, Duchene J, Zhang F, Zhang Z, Leung K-Y, Xiao Q, Scotland RS, Hodgkinson CP, Smith K, Willeit J, López-Otín C, Simpson IA, Kiechl S, Ahluwalia A, Xu Q, Ye S. A role of matrix metalloproteinase-8 in atherosclerosis. *Circ Res*. 2009;105:921–929.
- Quillard T, Araújo HA, Franck G, Tesmenitsky Y, Libby P. Matrix metalloproteinase-13 predominates over matrix metalloproteinase-8 as the functional interstitial collagenase in mouse atheromata. *Arterioscler Thromb Vasc Biol*. 2014;34:1179–1186.
- Sabeh F, Li XY, Saunders TL, Rowe RG, Weiss SJ. Secreted versus membrane-anchored collagenases: relative roles in fibroblast-dependent collagenolysis and invasion. *J Biol Chem*. 2009;284:23001–23011.
- Chun TH, Hotary KB, Sabeh F, Saltiel AR, Allen ED, Weiss SJ. A pericellular collagenase directs the 3-dimensional development of white adipose tissue. *Cell*. 2006;125:577–591.
- Holmbeck K, Bianco P, Caterina J, Yamada S, Kromer M, Kuznetsov SA, Mankani M, Robey PG, Poole AR, Pidoux I, Ward JM, Birkedal-Hansen H. MT1-MMP-deficient mice develop dwarfism, osteopenia, arthritis, and connective tissue disease due to inadequate collagen turnover. *Cell*. 1999;99:81–92.
- Zhou Z, Apte SS, Soininen R, Cao R, Baaklini GY, Rauser RW, Wang J, Cao Y, Tryggvason K. Impaired endochondral ossification and angiogenesis in mice deficient in membrane-type matrix metalloproteinase 1. *Proc Natl Acad Sci USA*. 2000;97:4052–4057.
- Schneider F, Sukhova GK, Aikawa M, Canner J, Gerdes N, Tang SM, Shi GP, Apte SS, Libby P. Matrix-metalloproteinase-14 deficiency in bone-marrow-derived cells promotes collagen accumulation in mouse atherosclerotic plaques. *Circulation*. 2008;117:931–939.
- Chun TH, Inoue M, Morisaki H, Yamanaka I, Miyamoto Y, Okamura T, Sato-Kusubata K, Weiss SJ. Genetic link between obesity and MMP14-dependent adipogenic collagen turnover. *Diabetes*. 2010;59:2484–2494.
- Filippov S, Koenig GC, Chun TH, Hotary KB, Ota I, Bugge TH, Roberts JD, Fay WP, Birkedal-Hansen H, Holmbeck K, Sabeh F, Allen ED, Weiss SJ. MT1-matrix metalloproteinase directs arterial wall invasion and neointima formation by vascular smooth muscle cells. *J Exp Med*. 2005;202:663–671.
- Piedrahita JA, Zhang SH, Hagaman JR, Oliver PM, Maeda N. Generation of mice carrying a mutant apolipoprotein E gene inactivated by gene targeting in embryonic stem cells. *Proc Natl Acad Sci USA*. 1992;89:4471–4475.
- Yana I, Sagara H, Takaki S, Takatsu K, Nakamura K, Nakao K, Katsuki M, Taniguchi S, Aoki T, Sato H, Weiss SJ, Seiki M. Crosstalk between neovessels and mural cells directs the site-specific expression of MT1-MMP to endothelial tip cells. *J Cell Sci*. 2007;120:1607–1614.
- Tang Y, Rowe RG, Botvinick EL, Kurup A, Putnam AJ, Seiki M, Weaver VM, Keller ET, Goldstein S, Dai J, Begun D, Saunders T, Weiss SJ. MT1-MMP-dependent control of skeletal stem cell commitment via a beta1-integrin/YAP/TAZ signaling axis. *Dev Cell*. 2013;25:402–416.
- Boucher P, Gotthardt M, Li WP, Anderson RG, Herz J. LRP: role in vascular wall integrity and protection from atherosclerosis. *Science*. 2003;300:329–332.
- Imai T, Takakuwa R, Marchand S, Dentz E, Bornert J-M, Messaddeq N, Wendling O, Mark M, Desvergne B, Wahli W, Chambon P, Metzger D. Peroxisome proliferator-activated receptor gamma is required in mature white and brown adipocytes for their survival in the mouse. *Proc Natl Acad Sci USA*. 2004;101:4543–4547.
- Öhman MK, Wright AP, Wickenheiser KJ, Luo W, Russo HM, Eitzman DT. Monocyte chemoattractant protein-1 deficiency protects against visceral fat-induced atherosclerosis. *Arterioscler Thromb Vasc Biol*. 2010;30:1151–1158.
- Maganto-García E, Tarrío M, Lichtman AH. Mouse models of atherosclerosis. *Curr Protoc Immunol*. 2001;Chapter 15:Unit 15.21.1–23.
- Chun TH, Inoue M. 3-D adipocyte differentiation and peri-adipocyte collagen turnover. *Methods Enzymol*. 2014;538:15–34.
- Lynn Ray J, Leach R, Herbert J-M, Benson M. Isolation of vascular smooth muscle cells from a single murine aorta. *Methods Cell Sci*. 2001;23:185–188.
- Afroze T, Husain M. C-Myb-binding sites mediate G1/S-associated repression of the plasma membrane Ca²⁺-ATPase-1 promoter. *J Biol Chem*. 2000;275:9062–9069.
- Moraes C, Labuz JM, Leung BM, Inoue M, Chun TH, Takayama S. On being the right size: scaling effects in designing a human-on-a-chip. *Integr Biol (Camb)*. 2013;5:1149–1161.
- Ford ES, Giles WH, Dietz WH. Prevalence of the metabolic syndrome among US adults: findings from the third National Health and Nutrition Examination Survey. *JAMA*. 2002;287:356–359.
- Chang L, Villacorta L, Li R, Hamblin M, Xu W, Dou C, Zhang J, Wu J, Zeng R, Chen YE. Loss of perivascular adipose tissue on peroxisome proliferator-

- activated receptor-gamma deletion in smooth muscle cells impairs intravascular thermoregulation and enhances atherosclerosis. *Circulation*. 2012;126:1067–1078.
29. Shen Z, Li C, Frieler RA, Gerasimova AS, Lee SJ, Wu J, Wang MM, Lumeng CN, Brosius FC, Duan SZ, Mortensen RM. Smooth muscle protein 22 alpha-Cre is expressed in myeloid cells in mice. *Biochem Biophys Res Commun*. 2012;422:639–642.
 30. Mott JD, Werb Z. Regulation of matrix biology by matrix metalloproteinases. *Curr Opin Cell Biol*. 2004;16:558–564.
 31. Gustafson B. Adipose tissue, inflammation and atherosclerosis. *J Atheroscler Thromb*. 2010;17:332–341.
 32. Ugrow EB, Slater S, Sala-Newby GB, Aguilera-Garcia CM, Angelini GD, Newby AC, George SJ. Dismantling of cadherin-mediated cell-cell contacts modulates smooth muscle cell proliferation. *Circ Res*. 2003;92:1314–1321.
 33. Koutsouki E, Beeching CA, Slater SC, Blaschuk OW, Sala-Newby GB, George SJ. N-cadherin-dependent cell-cell contacts promote human saphenous vein smooth muscle cell survival. *Arterioscler Thromb Vasc Biol*. 2005;25:982–988.
 34. Hou R, Liu L, Anees S, Hiroyasu S, Sibinga NES. The FAT1 cadherin integrates vascular smooth muscle cell growth and migration signals. *J Cell Biol*. 2006;173:417–429.
 35. Schlosser A, Pilecki B, Hemstra LE, Kejlving K, Kristmannsdottir GB, Wulf-Johansson H, Moeller JB, Fuchtbauer EM, Nielsen O, Kirketerp-Moller K, Dubey LK, Hansen PB, Stubbe J, Wrede C, Hegermann J, Ochs M, Rathkolb B, Schrewe A, Bekeredjian R, Wolf E, Gailus-Durner V, Fuchs H, Hrabe de Angelis M, Lindholt JS, Holmskov U, Sorensen GL. MFAP4 promotes vascular smooth muscle migration, proliferation and accelerates neointima formation. *Arterioscler Thromb Vasc Biol*. 2016;36:122–133.
 36. Ikesue M, Matsui Y, Ohta D, Danzaki K, Ito K, Kanayama M, Kurotaki D, Morimoto J, Kojima T, Tsutsui H, Ueda T. Syndecan-4 deficiency limits neointimal formation after vascular injury by regulating vascular smooth muscle cell proliferation and vascular progenitor cell mobilization. *Arterioscler Thromb Vasc Biol*. 2011;31:1066–1074.
 37. Ohuchi E, Imai K, Fujii Y, Sato H, Seiki M, Okada Y. Membrane type 1 matrix metalloproteinase digests interstitial collagens and other extracellular matrix macromolecules. *J Biol Chem*. 1997;272:2446–2451.
 38. Kajita M, Itoh Y, Chiba T, Mori H, Okada A, Kinoh H, Seiki M. Membrane-type 1 matrix metalloproteinase cleaves CD44 and promotes cell migration. *J Cell Biol*. 2001;153:893–904.
 39. Covington MD, Burghardt RC, Parrish AR. Ischemia-induced cleavage of cadherins in NRK cells requires MT1-MMP (MMP-14). *Am J Physiol Renal Physiol*. 2006;290:F43–F51.
 40. Moiseeva EP. Adhesion receptors of vascular smooth muscle cells and their functions. *Cardiovasc Res*. 2001;52:372–386.
 41. Shofuda K, Yasumitsu H, Nishihashi A, Miki K, Miyazaki K. Expression of three membrane-type matrix metalloproteinases (MT-MMPs) in rat vascular smooth muscle cells and characterization of MT3-MMP with and without transmembrane domain. *J Biol Chem*. 1997;272:9749–9754.
 42. Hotary K, Allen E, Punturieri A, Yana I, Weiss SJ. Regulation of cell invasion and morphogenesis in a three-dimensional type I collagen matrix by membrane-type matrix metalloproteinases 1, 2, and 3. *J Cell Biol*. 2000;149:1309–1323.
 43. Kothapalli D, Liu SL, Bae YH, Monslow J, Xu T, Hawthorne EA, Byfield FJ, Castagnino P, Rao S, Rader DJ, Puré E, Phillips MC, Lund-Katz S, Janney PA, Assoian RK. Cardiovascular protection by ApoE and ApoE-HDL linked to suppression of ECM gene expression and arterial stiffening. *Cell Rep*. 2012;2:1259–1271.
 44. Hong J-H, Hwang ES, McManus MT, Amsterdam A, Tian Y, Kalmukova R, Mueller E, Benjamin T, Spiegelman BM, Sharp PA, Hopkins N, Yaffe MB. TAZ, a transcriptional modulator of mesenchymal stem cell differentiation. *Science*. 2005;309:1074–1078.
 45. Dinardo CL, Venturini G, Zhou EH, Watanabe IS, Campos LC, Dariolli R, da Motta-Leal-Filho JM, Carvalho VM, Cardozo KH, Krieger JE, Alencar AM, Pereira AC. Variation of mechanical properties and quantitative proteomics of VSMC along the arterial tree. *Am J Physiol Heart Circ Physiol*. 2014;306:H505–H516.
 46. Shankman LS, Gomez D, Cherepanova OA, Salmon M, Alencar GF, Haskins RM, Swiatlowska P, Newman AAC, Greene ES, Straub AC, Isakson B, Randolph GJ, Owens GK. KLF4-dependent phenotypic modulation of smooth muscle cells has a key role in atherosclerotic plaque pathogenesis. *Nat Med*. 2015;21:628–637.
 47. Shimizu-Hirota R, Xiong W, Baxter BT, Kunkel SL, Maillard I, Chen X-Y, Sabe F, Liu R, Li X-Y, Weiss SJ. MT1-MMP-dependent regulation of a PI3K δ -nucleosome remodeling axis controls macrophage immune function. *Genes Dev*. 2012;26:395–413.

SUPPLEMENTAL MATERIAL

Table S1. List of genes differentially expressed in Cre(-) and SM22 α -Cre(+)Mmp14^{F/F} VSMCs

ENTREZ ID	SYMBOL	GENE NAME	Cre(-) 1	Cre(-) 2	Cre(+) 1	Cre(+) 2	Cre(-) AVG	Cre(+) AVG	Log2 (pos- nega)	Fold- change
379043	Raet1e	retinoic acid early transcript 1E	3.4	3.2	5.6	6.7	3.3	6.2	2.8	7.1
57266	Cxcl14	chemokine (C-X-C motif) ligand 14	5.4	4.7	8.6	6.4	5.0	7.5	2.5	5.7
20210	Saa3	serum amyloid A 3	3.4	6.0	7.3	7.0	4.7	7.1	2.5	5.5
14941	Gzmd	granzyme D	2.0	2.2	6.8	2.1	2.1	4.4	2.4	5.1
57781	Cd200r1	CD200 receptor 1	4.1	3.8	6.0	6.5	3.9	6.3	2.4	5.1
17533	Mrc1	mannose receptor, C type 1	4.9	5.7	7.0	7.7	5.3	7.4	2.1	4.2
80891	Fcrls	Fc receptor-like 5, scavenger receptor	6.0	3.7	8.2	5.6	4.8	6.9	2.1	4.2
232413	Clec12a	C-type lectin domain family 12, member a	4.8	5.3	7.3	6.8	5.0	7.0	2.0	4.1
56744	Pf4	platelet factor 4	4.3	5.2	5.5	8.1	4.8	6.8	2.0	4.1
21810	Tgfb1	transforming growth factor, beta induced	6.0	6.7	8.2	8.5	6.3	8.3	2.0	4.0
72318	Cyth4	cytohesin 4	5.8	5.7	7.6	7.9	5.8	7.7	2.0	3.9
15951	Ifi204	interferon activated gene 204	3.2	4.3	6.1	5.3	3.8	5.7	2.0	3.9
320292	Rasgef1b	RasGEF domain family, member 1B	3.7	3.9	5.8	5.7	3.8	5.8	2.0	3.9
12774	Ccr5	chemokine (C-C motif) receptor 5	3.4	3.0	4.8	5.4	3.2	5.1	1.9	3.7
14276	Folr2	folate receptor 2 (fetal)	5.0	4.5	8.0	5.4	4.8	6.7	1.9	3.7
20556	Sln2	schlafen 2	6.2	5.9	7.9	8.0	6.0	7.9	1.9	3.7
15109	Hal	histidine ammonia lyase	2.4	2.8	2.5	6.5	2.6	4.5	1.9	3.7
243277	Gpr133	G protein-coupled receptor 133	2.9	4.1	6.1	4.7	3.5	5.4	1.9	3.6
68774	Ms4a6d	membrane-spanning 4-domains, subfamily A, member 6D	5.7	5.6	7.5	7.5	5.6	7.5	1.8	3.6
17916	Myo1f	myosin IF	5.6	5.7	7.3	7.7	5.7	7.5	1.8	3.6
107321	Lpxn	leupaxin	3.2	3.7	5.5	5.0	3.4	5.2	1.8	3.5
246177	Myo1g	myosin IG	3.3	3.3	4.4	5.8	3.3	5.1	1.8	3.5
20452	St8sia4	ST8 alpha-N-acetylneuraminide alpha-2,8-sialyltransferase 4	4.0	4.5	5.7	6.3	4.3	6.0	1.8	3.4
109648	Npy	neuropeptide Y	8.0	7.5	8.9	10.1	7.7	9.5	1.8	3.4
17084	Ly86	lymphocyte antigen 86	4.3	5.5	6.2	7.0	4.9	6.6	1.8	3.4
19264	Ptpnc	protein tyrosine phosphatase, receptor type, C	6.6	6.7	8.3	8.5	6.6	8.4	1.8	3.4
13733	Emr1	EGF-like module containing, mucin-like, hormone receptor-like sequence 1	6.1	6.0	7.9	7.6	6.0	7.8	1.7	3.3
14727	Gp49a	glycoprotein 49 A	6.6	5.9	7.8	8.2	6.3	8.0	1.7	3.3
23845	Clec5a	C-type lectin domain family 5, member a	4.4	4.7	5.8	6.8	4.6	6.3	1.7	3.3
20568	Slpi	secretory leukocyte peptidase inhibitor	5.0	4.7	6.2	6.9	4.9	6.6	1.7	3.3

20308	Ccl9	chemokine (C-C motif) ligand 9	5.2	6.0	6.9	7.7	5.6	7.3	1.7	3.2
18733	Pirb	paired Ig-like receptor B	5.5	5.9	7.1	7.7	5.7	7.4	1.7	3.2
17060	Blk	B cell linker	6.1	6.1	7.8	7.8	6.1	7.8	1.7	3.2
100303646	AF357355	snoRNA AF357355	3.2	3.2	6.1	3.6	3.2	4.9	1.7	3.2
20288	Msr1	macrophage scavenger receptor 1	6.4	6.7	8.1	8.4	6.6	8.2	1.7	3.2
66109	Tspan13	tetraspanin 13	4.0	5.3	6.4	6.2	4.6	6.3	1.7	3.2
11501	Adam8	a disintegrin and metallopeptidase domain 8	6.6	6.5	8.3	8.0	6.5	8.2	1.7	3.1
319446	Dpep2	dipeptidase 2	5.3	3.9	6.6	5.9	4.6	6.3	1.7	3.1
544963	Iqgap2	IQ motif containing GTPase activating protein 2	5.4	4.9	6.3	7.3	5.2	6.8	1.6	3.1
69769	Tnfaip8l2	tumor necrosis factor, alpha-induced protein 8-like 2	4.6	4.9	6.1	6.8	4.8	6.4	1.6	3.1
12506	Cd48	CD48 antigen	5.8	5.3	6.9	7.5	5.6	7.2	1.6	3.1
382062	AB124611	cDNA sequence AB124611	5.1	5.1	6.3	7.1	5.1	6.7	1.6	3.1
15900	Irf8	interferon regulatory factor 8	5.5	5.2	6.6	7.3	5.4	7.0	1.6	3.1
20299	Ccl22	chemokine (C-C motif) ligand 22	2.7	3.3	2.6	6.7	3.0	4.6	1.6	3.0
20345	Selplg	selectin, platelet (p-selectin) ligand	5.5	5.1	6.3	7.5	5.3	6.9	1.6	3.0
22324	Vav1	vav 1 oncogene	4.5	3.8	5.6	5.9	4.2	5.8	1.6	3.0
16592	Fabp5	fatty acid binding protein 5, epidermal	8.5	8.0	9.4	10.2	8.2	9.8	1.6	3.0
17476	Mpeg1	macrophage expressed gene 1	6.9	6.6	8.0	8.7	6.8	8.3	1.6	3.0
233571	P2ry6	pyrimidinergic receptor P2Y, G-protein coupled, 6	6.9	6.6	8.5	8.2	6.7	8.3	1.6	3.0
15170	Ptpn6	protein tyrosine phosphatase, non-receptor type 6	5.0	5.3	6.4	7.1	5.2	6.7	1.6	3.0
83433	Trem2	triggering receptor expressed on myeloid cells 2	7.4	7.0	8.6	9.0	7.2	8.8	1.6	3.0
11690	Alox5ap	arachidonate 5-lipoxygenase activating protein	7.7	7.4	9.1	9.1	7.6	9.1	1.6	2.9
12259	C1qa	complement component 1, q subcomponent, alpha polypeptide	6.6	6.9	8.2	8.4	6.7	8.3	1.6	2.9
20302	Ccl3	chemokine (C-C motif) ligand 3	6.4	7.1	7.7	9.0	6.8	8.3	1.6	2.9
16912	Psmb9	proteasome (prosome, macropain) subunit, beta type 9 (large multifunctional peptidase 2)	4.6	4.8	5.8	6.7	4.7	6.3	1.6	2.9
14131	Fcgr3	Fc receptor, IgG, low affinity III	6.3	6.7	7.8	8.3	6.5	8.1	1.5	2.9
12768	Ccr1	chemokine (C-C motif) receptor 1	3.3	3.4	4.0	5.7	3.3	4.9	1.5	2.9
16149	Cd74	CD74 antigen (invariant polypeptide of major histocompatibility complex, class II antigen-associated)	3.9	3.4	3.7	6.6	3.6	5.1	1.5	2.9
17970	Ncf2	neutrophil cytosolic factor 2	5.2	5.6	6.5	7.4	5.4	7.0	1.5	2.9
17972	Ncf4	neutrophil cytosolic factor 4	3.6	4.3	5.2	5.8	4.0	5.5	1.5	2.9
14129	Fcgr1	Fc receptor, IgG, high affinity I	4.6	4.6	6.4	5.8	4.6	6.1	1.5	2.9
74272	1700054O19Rik	RIKEN cDNA 1700054O19 gene	2.5	4.0	4.8	4.7	3.2	4.7	1.5	2.8

12767	Cxcr4	chemokine (C-X-C motif) receptor 4	6.8	6.6	8.1	8.3	6.7	8.2	1.5	2.8
23900	Hcst	hematopoietic cell signal transducer	5.1	5.7	6.2	7.6	5.4	6.9	1.5	2.8
54712	Plxnc1	plexin C1	6.5	5.6	7.4	7.7	6.0	7.5	1.5	2.8
19354	Rac2	RAS-related C3 botulinum substrate 2	6.9	6.9	8.1	8.7	6.9	8.4	1.5	2.8
668218	Bin2	bridging integrator 2	3.0	2.9	3.9	5.0	2.9	4.4	1.5	2.8
217305	Cd300ld	CD300 molecule-like family member d	4.8	5.2	6.2	6.7	5.0	6.5	1.5	2.8
12984	Csf2rb2	colony stimulating factor 2 receptor, beta 2, low-affinity (granulocyte-macrophage)	6.3	6.0	7.3	8.0	6.1	7.6	1.5	2.8
13618	Ednrb	endothelin receptor type B	4.4	4.3	5.2	6.4	4.3	5.8	1.5	2.8
14130	Fcgr2b	Fc receptor, IgG, low affinity IIb	5.4	5.4	6.4	7.5	5.4	6.9	1.5	2.8
14544	Gda	guanine deaminase	4.8	5.9	6.3	7.4	5.4	6.8	1.5	2.8
14744	Gpr65	G-protein coupled receptor 65	5.8	4.9	7.1	6.7	5.4	6.9	1.5	2.8
66857	Plbd1	phospholipase B domain containing 1	3.2	4.9	3.2	7.8	4.0	5.5	1.5	2.8
16534	Kcnn4	potassium intermediate/small conductance calcium-activated channel, subfamily N, member 4	4.0	4.3	5.8	5.5	4.2	5.7	1.5	2.8
320207	Pik3r5	phosphoinositide-3-kinase, regulatory subunit 5, p101	5.9	5.7	7.2	7.4	5.8	7.3	1.5	2.8
216869	Arrb2	arrestin, beta 2	5.5	5.5	6.8	7.1	5.5	7.0	1.5	2.8
19735	Rgs2	regulator of G-protein signaling 2	5.3	4.4	6.2	6.5	4.9	6.3	1.5	2.8
217203	Tmem106a	transmembrane protein 106A	6.9	6.8	8.4	8.2	6.8	8.3	1.5	2.8
215632	Psd4	pleckstrin and Sec7 domain containing 4	4.1	2.9	4.7	5.1	3.5	4.9	1.5	2.7
226652	Arhgap30	Rho GTPase activating protein 30	4.8	4.6	5.8	6.4	4.7	6.1	1.4	2.7
12047	Bcl2a1d	B cell leukemia/lymphoma 2 related protein A1d	7.6	7.5	8.9	9.1	7.5	9.0	1.4	2.7
76933	Ifi2712a	interferon, alpha-inducible protein 27 like 2A	3.5	3.4	5.4	4.4	3.5	4.9	1.4	2.7
16197	Il7r	interleukin 7 receptor	6.7	7.2	7.8	9.0	7.0	8.4	1.4	2.7
17085	Ly9	lymphocyte antigen 9	4.1	4.3	5.2	6.1	4.2	5.7	1.4	2.7
105855	Nckap1l	NCK associated protein 1 like	6.9	6.8	8.2	8.4	6.8	8.3	1.4	2.7
239849	Cd200r4	CD200 receptor 4	6.6	6.2	7.7	8.0	6.4	7.9	1.4	2.7
16409	Itgam	integrin alpha M	5.7	5.9	6.4	8.0	5.8	7.2	1.4	2.7
50934	Slc7a8	solute carrier family 7 (cationic amino acid transporter, y+ system), member 8	5.9	5.8	7.2	7.4	5.9	7.3	1.4	2.7
107769	Tm6sf1	transmembrane 6 superfamily member 1	5.4	5.5	6.6	7.2	5.5	6.9	1.4	2.7
94176	Dock2	dedicator of cyto-kinesis 2	4.4	4.6	5.7	6.1	4.5	5.9	1.4	2.7
223433	Fam105a	family with sequence similarity 105, member A	5.1	5.0	6.1	6.8	5.1	6.5	1.4	2.7
279572	Tlr13	toll-like receptor 13	6.6	6.2	7.5	8.1	6.4	7.8	1.4	2.7

54486	Hpgds	hematopoietic prostaglandin D synthase	5.0	4.9	6.3	6.4	4.9	6.3	1.4	2.6
15559	Htr2b	5-hydroxytryptamine (serotonin) receptor 2B	3.8	4.2	5.3	5.6	4.0	5.4	1.4	2.6
11810	Apobec1	apolipoprotein B mRNA editing enzyme, catalytic polypeptide 1	7.3	7.4	8.8	8.7	7.3	8.7	1.4	2.6
17079	Cd180	CD180 antigen	6.9	6.7	8.3	8.0	6.8	8.2	1.4	2.6
13723	Emb	embigin	7.0	6.9	7.9	8.8	7.0	8.3	1.4	2.6
67092	Gatm	glycine amidinotransferase (L-arginine:glycine amidinotransferase)	4.8	4.9	5.7	6.8	4.9	6.2	1.4	2.6
382301	Sly	Sycp3 like Y-linked	4.4	4.9	6.3	5.9	4.7	6.1	1.4	2.6
27052	Aoah	acyloxyacyl hydrolase	3.4	3.2	4.4	5.0	3.3	4.7	1.4	2.6
20304	Ccl5	chemokine (C-C motif) ligand 5	4.7	5.3	5.1	7.6	5.0	6.4	1.4	2.6
12475	Cd14	CD14 antigen	5.6	5.8	7.1	7.0	5.7	7.1	1.4	2.6
246177	Myo1g	myosin IG	4.3	4.0	5.1	6.0	4.1	5.5	1.4	2.6
17969	Ncf1	neutrophil cytosolic factor 1	5.1	4.5	5.9	6.5	4.8	6.2	1.4	2.6
14960	H2-Aa	histocompatibility 2, class II antigen A, alpha	2.8	2.7	2.6	5.6	2.8	4.1	1.4	2.6
98496	Pid1	phosphotyrosine interaction domain containing 1	4.4	4.3	6.1	5.3	4.3	5.7	1.4	2.6
140497	AF251705	cDNA sequence AF251705	6.2	6.0	7.1	7.9	6.1	7.5	1.4	2.6
387142	Mir24-1	microRNA 24-1	3.3	4.0	5.6	4.5	3.7	5.0	1.4	2.6
67775	Rtp4	receptor transporter protein 4	3.1	2.7	5.4	3.0	2.9	4.2	1.4	2.6
12267	C3ar1	complement component 3a receptor 1	8.0	8.0	9.4	9.3	8.0	9.3	1.4	2.5
13032	Ctsc	cathepsin C	6.5	6.6	7.5	8.3	6.6	7.9	1.4	2.5
735268	Mir680-1	microRNA 680-1	4.4	5.8	6.7	6.2	5.1	6.4	1.3	2.5
50778	Rgs1	regulator of G-protein signaling 1	4.2	4.6	6.1	5.4	4.4	5.7	1.3	2.5
15442	Hpse	heparanase	5.4	5.7	6.3	7.4	5.5	6.9	1.3	2.5
56847	Aldh1a3	aldehyde dehydrogenase family 1, subfamily A3	4.6	4.0	6.2	5.0	4.3	5.6	1.3	2.5
12045	Bcl2a1b	B cell leukemia/lymphoma 2 related protein A1b	7.4	7.1	8.8	8.4	7.3	8.6	1.3	2.5
100628614	Mir5123	microRNA 5123	3.2	3.5	4.5	4.8	3.3	4.7	1.3	2.5
104759	Pld4	phospholipase D family, member 4	6.0	4.4	5.7	7.3	5.2	6.5	1.3	2.5
73329	1700040F15Rik	RIKEN cDNA 1700040F15 gene	4.4	5.6	6.5	6.1	5.0	6.3	1.3	2.5
68738	Acss1	acyl-CoA synthetase short-chain family member 1	2.7	3.4	3.8	4.9	3.1	4.4	1.3	2.5
52855	Lair1	leukocyte-associated Ig-like receptor 1	5.5	5.2	6.9	6.4	5.3	6.7	1.3	2.5
27419	Naglu	alpha-N-acetylglucosaminidase (Sanfilippo disease IIIB)	5.5	4.9	6.0	7.0	5.2	6.5	1.3	2.5
74039	Nfam1	Nfat activating molecule with ITAM motif 1	4.4	4.0	5.2	5.9	4.2	5.5	1.3	2.5
30955	Pik3cg	phosphoinositide-3-kinase, catalytic, gamma polypeptide	4.2	3.9	5.0	5.6	4.0	5.3	1.3	2.5
170744	Tlr8	toll-like receptor 8	4.8	4.6	5.6	6.4	4.7	6.0	1.3	2.5

210293	Dock10	dedicator of cytokinesis 10	5.9	5.7	6.5	7.7	5.8	7.1	1.3	2.5
212937	Tifab	TRAF-interacting protein with forkhead-associated domain, family member B	3.6	3.3	4.2	5.4	3.5	4.8	1.3	2.5
16411	Itgax	integrin alpha X	5.5	6.9	6.3	8.8	6.2	7.5	1.3	2.4
407790	Ndufa4l2	NADH dehydrogenase (ubiquinone) 1 alpha subcomplex, 4-like 2	3.6	6.2	6.3	6.1	4.9	6.2	1.3	2.4
16790	Anpep	alanyl (membrane) aminopeptidase	8.8	9.0	10.0	10.4	8.9	10.2	1.3	2.4
12044	Bcl2a1a	B cell leukemia/lymphoma 2 related protein A1a	6.0	6.3	7.2	7.6	6.2	7.4	1.3	2.4
18187	Nrp2	neuropilin 2	6.7	6.2	7.6	7.9	6.5	7.7	1.3	2.4
71653	4930506M07Rik	RIKEN cDNA 4930506M07 gene	6.1	5.5	6.4	7.7	5.8	7.1	1.3	2.4
60533	Cd274	CD274 antigen	4.7	4.5	4.6	7.1	4.6	5.8	1.3	2.4
18726	Lilra6	leukocyte immunoglobulin-like receptor, subfamily A (with TM domain), member 6	3.7	3.8	4.8	5.2	3.7	5.0	1.3	2.4
228026	Pdk1	pyruvate dehydrogenase kinase, isoenzyme 1	3.8	4.7	5.5	5.4	4.2	5.5	1.3	2.4
13034	Ctse	cathepsin E	3.0	4.3	3.2	6.7	3.7	4.9	1.3	2.4
15163	Hcls1	hematopoietic cell specific Lyn substrate 1	6.1	5.7	7.1	7.2	5.9	7.2	1.3	2.4
16822	Lcp2	lymphocyte cytosolic protein 2	5.3	5.3	6.2	6.9	5.3	6.5	1.3	2.4
237542	Osbp18	oxysterol binding protein-like 8	7.6	7.1	8.6	8.7	7.4	8.6	1.3	2.4
12523	Cd84	CD84 antigen	6.8	7.1	7.8	8.7	7.0	8.2	1.3	2.4
56619	Clec4e	C-type lectin domain family 4, member e	5.4	3.8	5.5	6.2	4.6	5.8	1.3	2.4
211228	Lrrc25	leucine rich repeat containing 25	3.9	4.3	5.0	5.7	4.1	5.3	1.3	2.4
12508	Cd53	CD53 antigen	8.5	8.5	9.6	10.0	8.5	9.8	1.2	2.4
83490	Pik3ap1	phosphoinositide-3-kinase adaptor protein 1	5.5	5.5	6.8	6.6	5.5	6.7	1.2	2.4
56193	Plek	pleckstrin	7.7	7.6	8.6	9.3	7.7	8.9	1.2	2.4
78591	A430104N18Rik	RIKEN cDNA A430104N18 gene	4.5	3.2	4.4	5.7	3.8	5.1	1.2	2.3
72042	Cotl1	coactosin-like 1 (Dictyostelium)	6.7	6.2	7.2	8.2	6.4	7.7	1.2	2.3
101056121	LOC101056121	Y-linked testis-specific protein 1-like	4.2	4.5	5.6	5.6	4.4	5.6	1.2	2.3
56857	Slc37a2	solute carrier family 37 (glycerol-3-phosphate transporter), member 2	5.2	4.7	6.2	6.2	5.0	6.2	1.2	2.3
170743	Tlr7	toll-like receptor 7	4.9	4.8	5.7	6.4	4.8	6.1	1.2	2.3
436467	Trav14-1	T cell receptor alpha variable 14-1	2.9	3.9	4.7	4.5	3.4	4.6	1.2	2.3
53314	Batf	basic leucine zipper transcription factor, ATF-like	3.8	3.7	4.5	5.4	3.7	4.9	1.2	2.3
12493	Cd37	CD37 antigen	4.9	4.7	5.9	6.2	4.8	6.1	1.2	2.3
16414	Itgb2	integrin beta 2	7.3	7.1	7.8	9.1	7.2	8.4	1.2	2.3
56792	Stap1	signal transducing adaptor family member 1	3.4	3.7	5.0	4.6	3.6	4.8	1.2	2.3
239393	Lrp12	low density lipoprotein-related protein 12	6.6	6.4	7.2	8.2	6.5	7.7	1.2	2.3

22368	Trpv2	transient receptor potential cation channel, subfamily V, member 2	6.1	5.6	7.0	7.1	5.8	7.0	1.2	2.3
100504230	AU020206	expressed sequence AU020206	8.0	7.0	8.5	8.8	7.5	8.7	1.2	2.3
212032	Hk3	hexokinase 3	3.8	4.0	5.0	5.2	3.9	5.1	1.2	2.3
80719	Igsf6	immunoglobulin superfamily, member 6	6.0	6.3	6.8	8.0	6.2	7.4	1.2	2.3
78771	Mctp1	multiple C2 domains, transmembrane 1	5.4	4.9	6.1	6.6	5.2	6.3	1.2	2.3
20564	Slit3	slit homolog 3 (Drosophila)	6.3	5.8	7.7	6.8	6.1	7.3	1.2	2.3
216991	Adap2	ArfGAP with dual PH domains 2	4.2	3.8	5.0	5.4	4.0	5.2	1.2	2.3
54725	Cadm1	cell adhesion molecule 1	6.9	5.7	7.4	7.6	6.3	7.5	1.2	2.3
18106	Cd244	CD244 natural killer cell receptor 2B4	3.0	2.8	3.3	4.9	2.9	4.1	1.2	2.3
16154	Il10ra	interleukin 10 receptor, alpha	3.8	4.0	4.8	5.3	3.9	5.1	1.2	2.3
101056060	LOC101056060	Y-linked testis-specific protein 1-like	4.8	5.5	6.4	6.2	5.1	6.3	1.2	2.3
23833	Cd52	CD52 antigen	7.1	6.9	7.7	8.7	7.0	8.2	1.2	2.3
12825	Col3a1	collagen, type III, alpha 1	5.5	5.4	7.0	6.2	5.4	6.6	1.2	2.3
66102	Cxcl16	chemokine (C-X-C motif) ligand 16	6.8	6.4	7.7	7.9	6.6	7.8	1.2	2.3
16331	Inpp5d	inositol polyphosphate-5-phosphatase D	5.8	5.3	6.6	6.9	5.6	6.7	1.2	2.3
68279	Mcoln2	mucoilin 2	5.3	4.4	6.0	6.1	4.9	6.0	1.2	2.3
109225	Ms4a7	membrane-spanning 4-domains, subfamily A, member 7	8.8	8.1	9.9	9.5	8.5	9.7	1.2	2.3
100034251	Wfdc17	WAP four-disulfide core domain 17	9.0	9.3	9.6	11.1	9.2	10.4	1.2	2.3
73149	Clec4a3	C-type lectin domain family 4, member a3	3.1	3.9	4.2	5.1	3.5	4.7	1.2	2.3
16658	Mafb	v-maf musculoaponeurotic fibrosarcoma oncogene family, protein B (avian)	4.9	4.7	5.9	6.1	4.8	6.0	1.2	2.3
245945	Rbm47	RNA binding motif protein 47	4.1	3.9	5.0	5.3	4.0	5.1	1.2	2.3
21938	Tnfrsf1b	tumor necrosis factor receptor superfamily, member 1b	6.8	6.5	7.3	8.4	6.7	7.8	1.2	2.3
57257	Vav3	vav 3 oncogene	3.4	3.0	4.3	4.4	3.2	4.3	1.2	2.3
219144	Arl11	ADP-ribosylation factor-like 11	4.9	4.6	5.7	6.1	4.7	5.9	1.2	2.2
12260	C1qb	complement component 1, q subcomponent, beta polypeptide	8.3	8.1	9.3	9.4	8.2	9.4	1.2	2.2
381654	C87414	expressed sequence C87414	2.3	4.2	4.3	4.6	3.3	4.4	1.2	2.2
108101	Fermt3	fermitin family homolog 3 (Drosophila)	4.6	4.6	5.7	5.9	4.6	5.8	1.2	2.2
207839	Galnt6	UDP-N-acetyl-alpha-D-galactosamine:polypeptide N-acetylgalactosaminyltransferase 6	4.9	4.5	5.4	6.3	4.7	5.9	1.2	2.2
18826	Lcp1	lymphocyte cytosolic protein 1	7.9	7.9	8.9	9.2	7.9	9.1	1.2	2.2
73656	Ms4a6c	membrane-spanning 4-domains, subfamily A, member 6C	4.3	3.8	4.6	5.8	4.1	5.2	1.2	2.2

22368	Trpv2	transient receptor potential cation channel, subfamily V, member 2	6.3	6.1	7.5	7.3	6.2	7.4	1.2	2.2
54445	Unc93b1	unc-93 homolog B1 (C. elegans)	6.6	6.2	7.3	7.8	6.4	7.6	1.2	2.2
12721	Coro1a	coronin, actin binding protein 1A	5.1	5.2	6.3	6.3	5.1	6.3	1.2	2.2
12978	Csf1r	colony stimulating factor 1 receptor	6.7	6.3	7.7	7.7	6.5	7.7	1.2	2.2
20311	Cxcl5	chemokine (C-X-C motif) ligand 5	3.5	4.3	4.6	5.5	3.9	5.1	1.2	2.2
13058	Cybb	cytochrome b-245, beta polypeptide	7.6	7.2	7.9	9.2	7.4	8.6	1.2	2.2
17948	Naip2	NLR family, apoptosis inhibitory protein 2	5.1	4.8	5.8	6.4	5.0	6.1	1.2	2.2
11468	Actg2	actin, gamma 2, smooth muscle, enteric	8.1	7.6	9.4	8.5	7.8	9.0	1.1	2.2
12491	Cd36	CD36 antigen	6.4	7.6	7.1	9.2	7.0	8.2	1.1	2.2
14017	Evi2a	ecotropic viral integration site 2a	5.7	5.7	6.8	6.8	5.7	6.8	1.1	2.2
23880	Fyb	FYN binding protein	5.5	5.0	6.7	6.2	5.3	6.4	1.1	2.2
70719	Hmha1	histocompatibility (minor) HA-1	4.8	4.0	5.6	5.5	4.4	5.5	1.1	2.2
64099	Parvg	parvin, gamma	3.5	3.9	3.7	5.8	3.7	4.8	1.1	2.2
230787	Themis2	thymocyte selection associated family member 2	4.5	4.3	5.1	6.0	4.4	5.5	1.1	2.2
57425	U90926	cDNA sequence U90926	3.9	5.3	4.8	6.7	4.6	5.7	1.1	2.2
12489	Cd33	CD33 antigen	6.0	5.7	5.7	8.2	5.8	7.0	1.1	2.2
14191	Fgr	Gardner-Rasheed feline sarcoma viral (Fgr) oncogene homolog	3.1	3.0	3.0	5.3	3.0	4.2	1.1	2.2
15117	Has2	hyaluronan synthase 2	5.3	5.3	6.4	6.5	5.3	6.5	1.1	2.2
14728	Lilrb4	leukocyte immunoglobulin-like receptor, subfamily B, member 4	9.1	9.5	10.3	10.6	9.3	10.4	1.1	2.2
69189	Mcemp1	mast cell expressed membrane protein 1	3.4	3.1	3.2	5.6	3.3	4.4	1.1	2.2
257662	Olf1290	olfactory receptor 1290	2.3	3.4	4.7	3.4	2.9	4.0	1.1	2.2
241452	Dhrs9	dehydrogenase/reductase (SDR family) member 9	4.0	4.2	5.2	5.3	4.1	5.3	1.1	2.2
56743	Lat2	linker for activation of T cells family, member 2	6.3	6.3	7.4	7.4	6.3	7.4	1.1	2.2
11846	Arg1	arginase, liver	3.8	3.4	4.3	5.2	3.6	4.7	1.1	2.2
665521	BC080696	cDNA sequence BC080696	3.5	4.0	4.7	5.0	3.7	4.8	1.1	2.2
18830	Pltp	phospholipid transfer protein	5.4	5.5	7.1	6.1	5.5	6.6	1.1	2.2
218442	Serinc5	serine incorporator 5	5.2	5.0	5.7	6.7	5.1	6.2	1.1	2.2
171209	Asic3	acid-sensing (proton-gated) ion channel 3	3.1	3.3	5.1	3.5	3.2	4.3	1.1	2.1
232975	Atp1a3	ATPase, Na ⁺ /K ⁺ transporting, alpha 3 polypeptide	5.6	5.3	6.0	7.2	5.5	6.6	1.1	2.1
20305	Ccl6	chemokine (C-C motif) ligand 6	6.6	7.8	6.5	10.1	7.2	8.3	1.1	2.1
329679	Fnip2	folliculin interacting protein 2	6.2	6.5	7.1	7.7	6.3	7.4	1.1	2.1
83924	Gpr137b	G protein-coupled receptor 137B	6.4	5.8	6.8	7.6	6.1	7.2	1.1	2.1

15950	Ifi203	interferon activated gene 203	3.4	3.1	5.0	3.7	3.2	4.3	1.1	2.1
213391	Rassf4	Ras association (RalGDS/AF-6) domain family member 4	4.6	3.4	4.9	5.3	4.0	5.1	1.1	2.1
76408	Abcc3	ATP-binding cassette, sub-family C (CFTR/MRP), member 3	5.0	4.2	5.9	5.5	4.6	5.7	1.1	2.1
620551	LOC620551	PRAME family member 5-like	3.3	3.9	4.8	4.5	3.6	4.7	1.1	2.1
20354	Sema4d	sema domain, immunoglobulin domain (Ig), transmembrane domain (TM) and short cytoplasmic domain, (semaphorin) 4D	4.3	4.1	5.1	5.4	4.2	5.3	1.1	2.1
20612	Siglec1	sialic acid binding Ig-like lectin 1, sialoadhesin	4.6	4.0	5.0	5.8	4.3	5.4	1.1	2.1
65221	Slc15a3	solute carrier family 15, member 3	7.3	7.4	8.1	8.8	7.3	8.4	1.1	2.1
320148	B430306N03Rik	RIKEN cDNA B430306N03 gene	4.2	4.1	4.7	5.7	4.1	5.2	1.1	2.1
12229	Btk	Bruton agammaglobulinemia tyrosine kinase	4.3	4.0	5.1	5.4	4.1	5.2	1.1	2.1
17474	Clec4d	C-type lectin domain family 4, member d	8.4	8.2	9.1	9.6	8.3	9.3	1.1	2.1
100316820	Mir1970	microRNA 1970	3.8	3.7	4.9	4.8	3.8	4.9	1.1	2.1
100628621	Mir3961	microRNA 3961	4.9	4.0	5.6	5.4	4.4	5.5	1.1	2.1
20611	Ssty1	spermiogenesis specific transcript on the Y 1	5.0	5.9	6.6	6.4	5.4	6.5	1.1	2.1
226409	Zranb3	zinc finger, RAN-binding domain containing 3	4.3	4.6	5.2	5.9	4.5	5.6	1.1	2.1
232201	Arhgap25	Rho GTPase activating protein 25	4.8	5.4	5.7	6.7	5.1	6.2	1.1	2.1
380732	Milr1	mast cell immunoglobulin like receptor 1	4.5	4.4	5.5	5.4	4.4	5.5	1.1	2.1
320024	Nceh1	neutral cholesterol ester hydrolase 1	8.0	7.9	8.9	9.2	8.0	9.0	1.1	2.1
14051	Eya4	eyes absent 4 homolog (Drosophila)	3.3	2.8	4.4	3.8	3.1	4.1	1.1	2.1
67731	Fbxo32	F-box protein 32	4.3	4.3	4.7	6.0	4.3	5.4	1.1	2.1
14176	Fgf5	fibroblast growth factor 5	4.1	3.8	4.4	5.6	3.9	5.0	1.1	2.1
237436	Gas2l3	growth arrest-specific 2 like 3	5.2	5.7	6.1	6.9	5.4	6.5	1.1	2.1
16114	Igk-V28	immunoglobulin kappa chain variable 28 (V28)	4.9	4.3	5.8	5.5	4.6	5.7	1.1	2.1
319480	Itga11	integrin alpha 11	4.0	4.0	6.1	4.0	4.0	5.1	1.1	2.1
320024	Nceh1	neutral cholesterol ester hydrolase 1	8.0	7.9	9.0	9.1	8.0	9.1	1.1	2.1
20846	Stat1	signal transducer and activator of transcription 1	5.9	5.6	7.2	6.5	5.8	6.8	1.1	2.1
12053	Bcl6	B cell leukemia/lymphoma 6	6.4	6.1	7.6	7.0	6.2	7.3	1.1	2.1
12606	Cebpa	CCAAT/enhancer binding protein (C/EBP), alpha	4.6	4.3	5.3	5.7	4.4	5.5	1.1	2.1
19141	Lgmn	legumain	8.4	8.3	9.3	9.4	8.3	9.4	1.1	2.1
241633	Atp8b4	ATPase, class I, type 8B, member 4	3.2	3.1	4.1	4.3	3.2	4.2	1.0	2.1
12362	Casp1	caspase 1	5.5	5.8	6.8	6.6	5.7	6.7	1.0	2.1
100628574	Mir28b	microRNA 28b	4.0	5.3	6.1	5.2	4.6	5.7	1.0	2.1

19200	Pstpip1	proline-serine-threonine phosphatase-interacting protein 1	5.0	5.3	5.9	6.4	5.1	6.2	1.0	2.1
18173	Slc11a1	solute carrier family 11 (proton-coupled divalent metal ion transporters), member 1	5.0	4.9	5.5	6.4	4.9	6.0	1.0	2.1
18636	Cfp	complement factor properdin	5.1	4.4	5.1	6.4	4.8	5.8	1.0	2.0
14127	Fcer1g	Fc receptor, IgE, high affinity I, gamma polypeptide	9.6	9.2	10.4	10.5	9.4	10.5	1.0	2.0
16186	Il2rg	interleukin 2 receptor, gamma chain	6.4	6.1	6.6	8.0	6.2	7.3	1.0	2.0
17101	Lyst	lysosomal trafficking regulator	5.5	5.6	6.3	6.9	5.6	6.6	1.0	2.0
667742	Piezo2	piezo-type mechanosensitive ion channel component 2	3.6	4.2	5.4	4.4	3.9	4.9	1.0	2.0
19332	Rab20	RAB20, member RAS oncogene family	4.4	4.1	5.4	5.2	4.3	5.3	1.0	2.0
11980	Atp8a1	ATPase, aminophospholipid transporter (APLT), class I, type 8A, member 1	3.6	3.4	4.2	4.8	3.5	4.5	1.0	2.0
14247	Fli1	Friend leukemia integration 1	5.4	5.4	6.2	6.7	5.4	6.4	1.0	2.0
211401	Mtss1	metastasis suppressor 1	6.6	6.5	7.7	7.4	6.5	7.6	1.0	2.0
17951	Naip5	NLR family, apoptosis inhibitory protein 5	4.1	3.5	4.1	5.5	3.8	4.8	1.0	2.0
241062	Pgap1	post-GPI attachment to proteins 1	5.2	5.4	5.6	7.1	5.3	6.3	1.0	2.0
19850	Rnu3a	U3A small nuclear RNA	3.2	3.3	4.2	4.3	3.2	4.3	1.0	2.0
69583	Tnfsf13	tumor necrosis factor (ligand) superfamily, member 13	6.0	6.0	6.8	7.3	6.0	7.0	1.0	2.0
20303	Ccl4	chemokine (C-C motif) ligand 4	5.7	6.1	6.9	6.9	5.9	6.9	1.0	2.0
12483	Cd22	CD22 antigen	3.7	3.8	4.1	5.5	3.8	4.8	1.0	2.0
234356	Csgalnact1	chondroitin sulfate N-acetylgalactosaminyltransferase 1	3.5	3.4	5.2	3.7	3.5	4.5	1.0	2.0
100041034	LOC100041034	Sp110 nuclear body protein-like	5.8	5.3	6.4	6.7	5.5	6.5	1.0	2.0
320139	Ptpn7	protein tyrosine phosphatase, non-receptor type 7	4.2	4.1	5.1	5.3	4.2	5.2	1.0	2.0
57319	Smpdl3a	sphingomyelin phosphodiesterase, acid-like 3A	6.7	6.4	7.3	7.9	6.6	7.6	1.0	2.0
652925	Tmem243	transmembrane protein 243, mitochondrial	3.8	4.2	4.8	5.3	4.0	5.0	1.0	2.0
12262	C1qc	complement component 1, q subcomponent, C chain	7.1	7.2	8.1	8.1	7.1	8.1	1.0	2.0
101056308	LOC101056308	Y-linked testis-specific protein 1-like	3.5	3.9	4.9	4.5	3.7	4.7	1.0	2.0
140795	P2ry14	purinergic receptor P2Y, G-protein coupled, 14	3.2	3.7	3.6	5.3	3.5	4.5	1.0	2.0
11835	Ar	androgen receptor	5.1	4.9	3.8	4.1	5.0	4.0	-1.0	-2.0
19716	Bex1	brain expressed gene 1	5.7	6.4	3.2	6.9	6.1	5.1	-1.0	-2.0
241520	Fam171b	family with sequence similarity 171, member B	4.3	4.8	3.5	3.6	4.5	3.5	-1.0	-2.0
18481	Pak3	p21 protein (Cdc42/Rac)-activated kinase 3	4.8	4.7	3.8	3.7	4.7	3.7	-1.0	-2.0

76969	Chst1	carbohydrate (keratan sulfate Gal-6) sulfotransferase 1	4.6	4.6	3.9	3.2	4.6	3.6	-1.0	-2.0
71785	Pdgfd	platelet-derived growth factor, D polypeptide	6.6	5.9	5.6	4.8	6.2	5.2	-1.0	-2.0
20289	Scx	scleraxis	3.4	4.8	2.8	3.3	4.1	3.1	-1.0	-2.0
21873	Tjp2	tight junction protein 2	6.6	6.2	5.3	5.4	6.4	5.4	-1.0	-2.0
217310	Hid1	HID1 domain containing	4.7	5.0	3.7	3.9	4.8	3.8	-1.0	-2.0
100604	Lrrc8c	leucine rich repeat containing 8 family, member C	8.2	8.1	6.6	7.7	8.2	7.1	-1.0	-2.0
14013	Mecom	MDS1 and EVI1 complex locus	4.1	4.1	3.1	3.0	4.1	3.1	-1.0	-2.0
235505	Cd109	CD109 antigen	7.0	8.2	6.4	6.7	7.6	6.6	-1.0	-2.1
12583	Cdo1	cysteine dioxygenase 1, cytosolic	7.9	8.6	7.1	7.3	8.2	7.2	-1.0	-2.1
13874	Ereg	epiregulin	8.7	8.3	7.2	7.8	8.5	7.5	-1.0	-2.1
22762	Zfpm2	zinc finger protein, multitype 2	5.7	5.4	4.7	4.3	5.5	4.5	-1.0	-2.1
18214	Ddr2	discoidin domain receptor family, member 2	7.5	7.4	6.9	6.0	7.5	6.4	-1.1	-2.1
74754	Dhcr24	24-dehydrocholesterol reductase	7.4	7.5	6.7	6.1	7.5	6.4	-1.1	-2.1
66203	Lce1m	late cornified envelope 1M	5.3	4.6	3.9	3.9	4.9	3.9	-1.1	-2.1
19223	Ptgis	prostaglandin I2 (prostacyclin) synthase	7.5	8.2	6.7	6.9	7.8	6.8	-1.1	-2.1
216363	Rab3ip	RAB3A interacting protein	7.4	7.5	6.6	6.1	7.4	6.4	-1.1	-2.1
24052	Sgcd	sarcoglycan, delta (dystrophin-associated glycoprotein)	5.7	5.7	4.5	4.8	5.7	4.7	-1.1	-2.1
20983	Syt4	synaptotagmin IV	5.9	3.3	3.5	3.5	4.6	3.5	-1.1	-2.1
11752	Anxa8	annexin A8	4.6	4.6	3.7	3.4	4.6	3.6	-1.1	-2.1
14457	Gas7	growth arrest specific 7	6.1	5.8	4.4	5.4	5.9	4.9	-1.1	-2.1
69884	2010300F17Rik	RIKEN cDNA 2010300F17 gene	5.8	4.3	4.0	3.9	5.0	4.0	-1.1	-2.1
320692	9430037G07Rik	RIKEN cDNA 9430037G07 gene	5.4	3.9	3.5	3.6	4.6	3.6	-1.1	-2.1
20315	Cxcl12	chemokine (C-X-C motif) ligand 12	9.1	10.1	8.6	8.5	9.6	8.5	-1.1	-2.1
207683	Igsf11	immunoglobulin superfamily, member 11	6.8	6.6	5.0	6.3	6.7	5.6	-1.1	-2.1
107065	Lrrtm2	leucine rich repeat transmembrane neuronal 2	4.2	4.6	3.2	3.5	4.4	3.3	-1.1	-2.1
68458	Ppp1r14a	protein phosphatase 1, regulatory (inhibitor) subunit 14A	4.6	3.4	3.2	2.8	4.0	3.0	-1.1	-2.1
240725	Sulf1	sulfatase 1	9.3	9.5	8.7	8.0	9.4	8.4	-1.1	-2.1
69953	2810025M15Rik	RIKEN cDNA 2810025M15 gene	7.2	8.0	6.4	6.7	7.6	6.5	-1.1	-2.1
68567	Cgref1	cell growth regulator with EF hand domain 1	6.3	6.0	4.9	5.3	6.2	5.1	-1.1	-2.1
15551	Htr1b	5-hydroxytryptamine (serotonin) receptor 1B	6.2	5.6	4.7	5.0	5.9	4.8	-1.1	-2.1
381493	S100a7a	S100 calcium binding protein A7A	6.1	4.9	4.1	4.8	5.5	4.4	-1.1	-2.1
56496	Tspan6	tetraspanin 6	8.3	7.6	7.1	6.6	7.9	6.8	-1.1	-2.1
70892	Ttll7	tubulin tyrosine ligase-like family, member 7	5.5	6.1	4.8	4.7	5.8	4.7	-1.1	-2.1

14266	Aff2	AF4/FMR2 family, member 2	5.5	5.2	4.7	3.8	5.4	4.3	-1.1	-2.1
104943	Fam110c	family with sequence similarity 110, member C	4.6	4.2	3.3	3.3	4.4	3.3	-1.1	-2.1
14205	Figf	c-fos induced growth factor	6.3	7.3	6.6	4.9	6.8	5.8	-1.1	-2.1
20378	Frzb	frizzled-related protein	6.6	7.7	6.4	5.6	7.1	6.0	-1.1	-2.1
16447	Ivl	involucrin	6.5	4.3	4.0	4.6	5.4	4.3	-1.1	-2.1
21956	Tnnt2	troponin T2, cardiac	5.7	5.8	4.3	5.0	5.8	4.7	-1.1	-2.1
12269	C4bp	complement component 4 binding protein	4.9	4.8	4.1	3.4	4.9	3.8	-1.1	-2.1
12389	Cav1	caveolin 1, caveolae protein	8.1	7.7	6.6	6.9	7.9	6.8	-1.1	-2.1
73379	Dcbl2	discoidin, CUB and LCCL domain containing 2	7.4	6.9	6.5	5.6	7.1	6.0	-1.1	-2.1
67350	1700084E18Rik	RIKEN cDNA 1700084E18 gene	4.8	3.9	3.1	3.4	4.3	3.2	-1.1	-2.2
66175	Mustn1	musculoskeletal, embryonic nuclear protein 1	9.8	8.6	8.7	7.5	9.2	8.1	-1.1	-2.2
269233	Fam171a1	family with sequence similarity 171, member A1	6.3	6.6	5.1	5.6	6.4	5.3	-1.1	-2.2
329628	Fat4	FAT tumor suppressor homolog 4 (Drosophila)	5.2	5.2	4.2	4.1	5.2	4.1	-1.1	-2.2
77446	Heg1	HEG homolog 1 (zebrafish)	7.7	8.2	7.4	6.3	7.9	6.8	-1.1	-2.2
100503380	Snhg4	small nucleolar RNA host gene 4	4.7	4.2	3.1	3.4	4.4	3.3	-1.1	-2.2
23876	Fbln5	fibulin 5	8.4	8.9	8.2	6.8	8.6	7.5	-1.1	-2.2
16008	Igfbp2	insulin-like growth factor binding protein 2	6.5	7.8	6.7	5.4	7.2	6.1	-1.1	-2.2
233726	Ipo7	importin 7	7.9	7.4	6.5	6.5	7.6	6.5	-1.1	-2.2
13642	Efnb2	ephrin B2	7.8	7.7	6.6	6.7	7.8	6.6	-1.1	-2.2
67374	Jam2	junction adhesion molecule 2	8.8	9.2	7.8	7.9	9.0	7.9	-1.1	-2.2
68404	Nrn1	neuritin 1	7.1	7.6	5.4	7.0	7.4	6.2	-1.1	-2.2
71720	Osbpl3	oxysterol binding protein-like 3	4.8	5.0	3.4	4.1	4.9	3.7	-1.1	-2.2
19243	Ptp4a1	protein tyrosine phosphatase 4a1	6.4	5.8	4.6	5.4	6.1	5.0	-1.1	-2.2
72780	Rspo3	R-spondin 3 homolog (Xenopus laevis)	6.2	6.4	6.0	4.4	6.3	5.2	-1.1	-2.2
217410	Trib2	tribbles homolog 2 (Drosophila)	5.9	6.3	5.3	4.6	6.1	4.9	-1.1	-2.2
12064	Bdnf	brain derived neurotrophic factor	5.6	5.2	4.5	4.0	5.4	4.3	-1.2	-2.2
14677	Gnai1	guanine nucleotide binding protein (G protein), alpha inhibiting 1	6.3	7.0	5.6	5.5	6.7	5.5	-1.2	-2.2
22160	Twist1	twist basic helix-loop-helix transcription factor 1	6.1	6.5	5.3	5.0	6.3	5.1	-1.2	-2.2
73720	Cst6	cystatin E/M	5.4	5.3	4.3	4.1	5.3	4.2	-1.2	-2.2
319146	Ifnz	interferon zeta	5.2	4.5	3.8	3.7	4.9	3.7	-1.2	-2.2
23959	Nt5e	5' nucleotidase, ecto	4.7	4.3	3.1	3.5	4.5	3.3	-1.2	-2.3
19272	Ptprk	protein tyrosine phosphatase, receptor type, K	7.0	6.9	5.6	6.0	7.0	5.8	-1.2	-2.3
20197	S100a3	S100 calcium binding protein A3	5.3	5.1	3.9	4.1	5.2	4.0	-1.2	-2.3

100217453	Snord16a	small nucleolar RNA, C/D box 16A	7.0	6.5	5.3	5.8	6.7	5.6	-1.2	-2.3
11421	Ace	angiotensin I converting enzyme (peptidyl-dipeptidase A) 1	3.4	4.8	2.9	2.9	4.1	2.9	-1.2	-2.3
170757	Elt1	EGF, latrophilin seven transmembrane domain containing 1	5.1	3.6	3.1	3.2	4.4	3.2	-1.2	-2.3
53614	Reck	reversion-inducing-cysteine-rich protein with kazal motifs	6.9	7.4	6.1	5.8	7.2	6.0	-1.2	-2.3
58994	Smpd3	sphingomyelin phosphodiesterase 3, neutral	5.4	4.4	3.8	3.7	4.9	3.7	-1.2	-2.3
13797	Emx2	empty spiracles homeobox 2	5.2	4.0	3.7	3.1	4.6	3.4	-1.2	-2.3
16773	Lama2	laminin, alpha 2	6.2	6.3	5.0	5.1	6.3	5.1	-1.2	-2.3
17386	Mmp13	matrix metalloproteinase 13	8.3	9.1	6.8	8.1	8.7	7.5	-1.2	-2.3
22329	Vcam1	vascular cell adhesion molecule 1	8.2	8.3	7.2	6.9	8.2	7.0	-1.2	-2.3
217887	BC022687	cDNA sequence BC022687	6.7	6.6	5.4	5.4	6.6	5.4	-1.2	-2.3
19224	Ptgs1	prostaglandin-endoperoxide synthase 1	7.1	7.8	5.9	6.5	7.4	6.2	-1.2	-2.3
14611	Gja3	gap junction protein, alpha 3	5.1	3.5	3.2	2.8	4.3	3.0	-1.2	-2.3
13876	Erg	avian erythroblastosis virus E-26 (v-ets) oncogene related	4.6	4.4	3.2	3.3	4.5	3.3	-1.2	-2.3
16669	Krt19	keratin 19	4.5	4.6	3.4	3.3	4.6	3.3	-1.2	-2.3
216459	Myl6b	myosin, light polypeptide 6B	5.6	5.5	4.5	4.2	5.6	4.3	-1.2	-2.3
18788	Serpinb2	serine (or cysteine) peptidase inhibitor, clade B, member 2	7.8	6.1	4.1	7.3	6.9	5.7	-1.2	-2.3
20042	Rps12	ribosomal protein S12	4.9	4.6	3.3	3.7	4.7	3.5	-1.2	-2.4
97848	Serpinb6c	serine (or cysteine) peptidase inhibitor, clade B, member 6c	7.1	5.7	5.7	4.5	6.4	5.1	-1.3	-2.4
23967	Osr1	odd-skipped related 1 (Drosophila)	7.9	9.0	7.6	6.8	8.5	7.2	-1.3	-2.4
16367	Irs1	insulin receptor substrate 1	6.2	5.7	4.8	4.6	6.0	4.7	-1.3	-2.4
13395	Dlx5	distal-less homeobox 5	3.0	5.2	3.0	2.6	4.1	2.8	-1.3	-2.4
110454	Ly6a	lymphocyte antigen 6 complex, locus A	8.1	10.1	8.1	7.6	9.1	7.9	-1.3	-2.4
73904	4833412C05Rik	RIKEN cDNA 4833412C05 gene	5.9	4.9	3.9	4.3	5.4	4.1	-1.3	-2.4
14461	Gata2	GATA binding protein 2	4.7	4.3	3.3	3.1	4.5	3.2	-1.3	-2.5
279653	Pcdh19	protocadherin 19	7.3	6.7	5.9	5.6	7.0	5.7	-1.3	-2.5
109294	Prex2	phosphatidylinositol-3,4,5-trisphosphate-dependent Rac exchange factor 2	5.5	5.5	4.3	4.1	5.5	4.2	-1.3	-2.5
229672	Bcl2l15	BCL2-like 15	5.4	4.9	3.1	4.7	5.2	3.9	-1.3	-2.5
216616	Efemp1	epidermal growth factor-containing fibulin-like extracellular matrix protein 1	7.9	9.6	7.8	7.1	8.8	7.5	-1.3	-2.5
11668	Aldh1a1	aldehyde dehydrogenase family 1, subfamily A1	7.8	7.0	6.6	5.5	7.4	6.1	-1.3	-2.5
407828	BC023969	cDNA sequence BC023969	3.8	5.7	3.3	3.5	4.7	3.4	-1.3	-2.5
216831	Arhgap44	Rho GTPase activating protein 44	6.4	6.4	5.3	4.9	6.4	5.1	-1.3	-2.5
211323	Nrg1	neuregulin 1	6.6	5.6	4.8	4.7	6.1	4.8	-1.3	-2.5

16398	Itga2	integrin alpha 2	6.5	6.7	4.6	5.8	6.6	5.2	-1.4	-2.6
433619	Kprp	keratinocyte expressed, proline-rich	7.2	5.5	5.0	4.8	6.3	4.9	-1.4	-2.7
27273	Pdk4	pyruvate dehydrogenase kinase, isoenzyme 4	7.5	6.6	5.5	5.8	7.1	5.6	-1.4	-2.7
94242	Tinagl1	tubulointerstitial nephritis antigen-like 1	6.7	7.3	5.5	5.7	7.0	5.6	-1.4	-2.7
14600	Ghr	growth hormone receptor	7.7	7.4	6.3	6.1	7.6	6.2	-1.4	-2.7
73738	Haus7	HAUS augmin-like complex, subunit 7	5.6	6.4	4.7	4.5	6.0	4.6	-1.4	-2.7
15483	Hsd11b1	hydroxysteroid 11-beta dehydrogenase 1	5.3	7.2	5.0	4.6	6.2	4.8	-1.4	-2.7
29818	Hspb7	heat shock protein family, member 7 (cardiovascular)	7.6	8.1	6.4	6.4	7.9	6.4	-1.4	-2.7
11731	Ang2	angiogenin, ribonuclease A family, member 2	7.4	7.7	5.9	6.2	7.5	6.0	-1.5	-2.8
12161	Bmp6	bone morphogenetic protein 6	5.0	4.8	3.6	3.2	4.9	3.4	-1.5	-2.8
73173	Pcdh18	protocadherin 18	6.8	6.1	5.2	4.8	6.4	5.0	-1.5	-2.8
223881	Rnd1	Rho family GTPase 1	5.8	6.1	4.5	4.5	6.0	4.5	-1.5	-2.8
110058	Syt17	synaptotagmin XVII	7.0	7.0	5.2	5.9	7.0	5.5	-1.5	-2.8
54195	Gucy1b3	guanylate cyclase 1, soluble, beta 3	6.2	5.3	4.1	4.4	5.8	4.3	-1.5	-2.8
19124	Procr	protein C receptor, endothelial	8.0	6.8	5.8	6.1	7.4	5.9	-1.5	-2.8
654795	Sdr39u1	short chain dehydrogenase/reductase family 39U, member 1	7.1	4.8	4.1	4.9	6.0	4.5	-1.5	-2.8
56429	Dpt	dermatopontin	6.9	5.8	4.4	5.3	6.4	4.8	-1.5	-2.8
224792	Gpr116	G protein-coupled receptor 116	4.9	4.3	3.0	3.1	4.6	3.1	-1.5	-2.9
26415	Mapk13	mitogen-activated protein kinase 13	6.6	6.6	4.8	5.4	6.6	5.1	-1.5	-2.9
18383	Tnfrsf11b	tumor necrosis factor receptor superfamily, member 11b (osteoprotegerin)	7.6	7.9	6.5	6.0	7.8	6.2	-1.5	-2.9
13024	Ctla2a	cytotoxic T lymphocyte- associated protein 2 alpha	9.5	8.7	7.9	7.2	9.1	7.6	-1.5	-2.9
76400	Pbp2	phosphatidylethanolamine binding protein 2	5.7	4.6	4.0	3.2	5.1	3.6	-1.5	-2.9
228765	Sdcbp2	syndecan binding protein (syntenin) 2	7.0	5.4	4.7	4.6	6.2	4.7	-1.5	-2.9
20706	Serpib9b	serine (or cysteine) peptidase inhibitor, clade B, member 9b	9.4	9.1	8.0	7.4	9.2	7.7	-1.5	-2.9
12484	Cd24a	CD24a antigen	9.4	8.5	6.3	8.6	9.0	7.4	-1.6	-3.0
14858	Gsta2	glutathione S-transferase, alpha 2 (Yc2)	5.7	6.1	4.4	4.2	5.9	4.3	-1.6	-3.0
20682	Sox9	SRY (sex determining region Y)- box 9	5.1	6.6	3.9	4.6	5.8	4.2	-1.6	-3.0
22634	Plagl1	pleiomorphic adenoma gene- like 1	5.6	6.3	3.5	5.2	6.0	4.4	-1.6	-3.0
12349	Car2	carbonic anhydrase 2	6.1	5.2	3.8	4.3	5.7	4.0	-1.6	-3.1
268977	Ltbp1	latent transforming growth factor beta binding protein 1	6.7	7.4	5.2	5.6	7.0	5.4	-1.6	-3.1
13614	Edn1	endothelin 1	8.8	7.8	6.6	6.8	8.3	6.7	-1.7	-3.2

13640	Efna5	ephrin A5	6.2	6.6	4.3	5.1	6.4	4.7	-1.7	-3.2
11459	Acta1	actin, alpha 1, skeletal muscle	8.8	7.7	5.6	7.6	8.2	6.6	-1.7	-3.2
232431	Gprc5a	G protein-coupled receptor, family C, group 5, member A	4.6	4.8	2.6	3.4	4.7	3.0	-1.7	-3.2
68178	Cgnl1	cingulin-like 1	7.7	7.3	5.6	6.1	7.5	5.8	-1.7	-3.2
68052	Rps13	ribosomal protein S13	4.3	4.5	2.6	2.8	4.4	2.7	-1.7	-3.2
11435	Chrna1	cholinergic receptor, nicotinic, alpha polypeptide 1 (muscle)	3.7	5.1	2.7	2.7	4.4	2.7	-1.7	-3.3
14368	Fzd6	frizzled homolog 6 (Drosophila)	5.8	4.7	3.4	3.6	5.2	3.5	-1.7	-3.3
16400	Itga3	integrin alpha 3	5.4	5.1	3.3	3.7	5.2	3.5	-1.7	-3.3
64058	Perp	PERP, TP53 apoptosis effector	6.2	5.0	3.9	3.9	5.6	3.9	-1.7	-3.3
17389	Mmp16	matrix metalloproteinase 16	4.7	5.1	3.3	3.1	4.9	3.2	-1.7	-3.3
320092	E030003E18Rik	RIKEN cDNA E030003E18 gene	5.9	5.1	4.5	3.1	5.5	3.8	-1.8	-3.4
224093	Fam43a	family with sequence similarity 43, member A	6.3	6.6	5.2	4.2	6.5	4.7	-1.8	-3.4
20324	Sdpr	serum deprivation response	8.9	9.5	7.5	7.4	9.2	7.4	-1.8	-3.4
13717	Eln	elastin	5.1	6.6	4.0	4.1	5.8	4.0	-1.8	-3.5
67718	Lce1h	late cornified envelope 1H	7.7	3.3	3.7	3.7	5.5	3.7	-1.8	-3.5
20708	Serpinb6b	serine (or cysteine) peptidase inhibitor, clade B, member 6b	8.3	7.9	6.7	5.9	8.1	6.3	-1.8	-3.5
14725	Lrp2	low density lipoprotein receptor-related protein 2	5.2	4.1	2.8	2.9	4.7	2.8	-1.8	-3.5
16891	Lipg	lipase, endothelial	5.0	4.6	2.7	3.2	4.8	3.0	-1.8	-3.6
67828	Lce1f	late cornified envelope 1F	7.2	3.1	3.3	3.2	5.1	3.3	-1.9	-3.6
18104	Nqo1	NAD(P)H dehydrogenase, quinone 1	7.3	7.4	5.0	5.9	7.3	5.5	-1.9	-3.7
105450	Mmrn2	multimerin 2	6.3	5.3	3.7	4.1	5.8	3.9	-1.9	-3.8
71690	Esm1	endothelial cell-specific molecule 1	8.1	8.2	5.9	6.5	8.2	6.2	-1.9	-3.8
94253	Hecw1	HECT, C2 and WW domain containing E3 ubiquitin protein ligase 1	6.1	4.9	3.8	3.2	5.5	3.5	-2.0	-4.1
105349	Akr1c18	aldo-keto reductase family 1, member C18	5.6	8.0	4.0	5.3	6.8	4.7	-2.1	-4.3
101772	Ano1	anoctamin 1, calcium activated chloride channel	5.1	4.7	2.7	2.8	4.9	2.7	-2.1	-4.4
21892	Tll1	tolloid-like	8.4	8.0	5.6	6.5	8.2	6.1	-2.1	-4.4
69325	1700012B09Rik	RIKEN cDNA 1700012B09 gene	5.8	6.9	3.7	4.5	6.4	4.1	-2.3	-4.9
12159	Bmp4	bone morphogenetic protein 4	7.5	7.8	6.6	4.1	7.7	5.4	-2.3	-5.1
319154	Hist2h3b	histone cluster 2, H3b	6.2	4.5	2.5	3.5	5.4	3.0	-2.4	-5.2
22268	Upk1b	uroplakin 1B	9.2	5.8	4.3	5.9	7.5	5.1	-2.4	-5.2
12490	Cd34	CD34 antigen	7.0	5.8	3.5	4.5	6.4	4.0	-2.4	-5.3
114301	Palmd	palmdelphin	6.1	5.2	3.3	3.1	5.6	3.2	-2.4	-5.4
20344	Selp	selectin, platelet	6.3	6.5	3.9	4.1	6.4	4.0	-2.5	-5.5
59308	Emcn	endomucin	9.3	8.1	6.0	6.5	8.7	6.2	-2.5	-5.6
18613	Pecam1	platelet/endothelial cell adhesion molecule 1	6.7	6.3	3.9	4.1	6.5	4.0	-2.5	-5.6

12562	Cdh5	cadherin 5	8.7	7.0	5.0	5.7	7.8	5.3	-2.5	-5.7
18812	Prl2c3	prolactin family 2, subfamily c, member 3	9.5	9.0	6.4	6.6	9.2	6.5	-2.7	-6.6
18812	Prl2c3	prolactin family 2, subfamily c, member 3	9.3	9.0	6.2	6.6	9.1	6.4	-2.7	-6.7
223272	Itgbl1	integrin, beta-like 1	7.6	7.7	4.5	5.2	7.6	4.9	-2.8	-6.7
76294	Asb5	ankyrin repeat and SOCs box-containing 5	7.8	6.9	3.7	5.4	7.3	4.6	-2.8	-6.8
240873	Tnfsf18	tumor necrosis factor (ligand) superfamily, member 18	9.1	7.0	4.5	6.0	8.0	5.2	-2.8	-7.1
20753	Sprr1a	small proline-rich protein 1A	8.6	9.6	5.4	7.1	9.1	6.2	-2.8	-7.2
19263	Ptprb	protein tyrosine phosphatase, receptor type, B	6.5	6.4	3.7	3.5	6.4	3.6	-2.9	-7.4
228576	Mall	mal, T cell differentiation protein-like	8.2	5.7	4.4	3.6	7.0	4.0	-3.0	-7.9
72381	2210409E12Rik	transcription elongation factor B (SIII), polypeptide 2 pseudogene	6.4	6.0	4.0	2.3	6.2	3.2	-3.0	-8.1
12319	Car8	carbonic anhydrase 8	7.3	7.2	4.4	4.0	7.2	4.2	-3.0	-8.1
68632	Myct1	myc target 1	7.4	6.7	3.9	4.2	7.1	4.0	-3.0	-8.1
74175	Crct1	cysteine-rich C-terminal 1	6.6	6.4	3.1	3.8	6.5	3.4	-3.1	-8.3
224796	Clic5	chloride intracellular channel 5	6.4	6.9	2.9	3.1	6.7	3.0	-3.7	-12.6

Figure S1. Arterial trees dissected from *Cre(-)*, *SM22 α -Cre(+)*, and *aP2-Cre(+)* *MMP14^{F/F}Apoe^{-/-}* male and female mice after a 12-week Western diet.

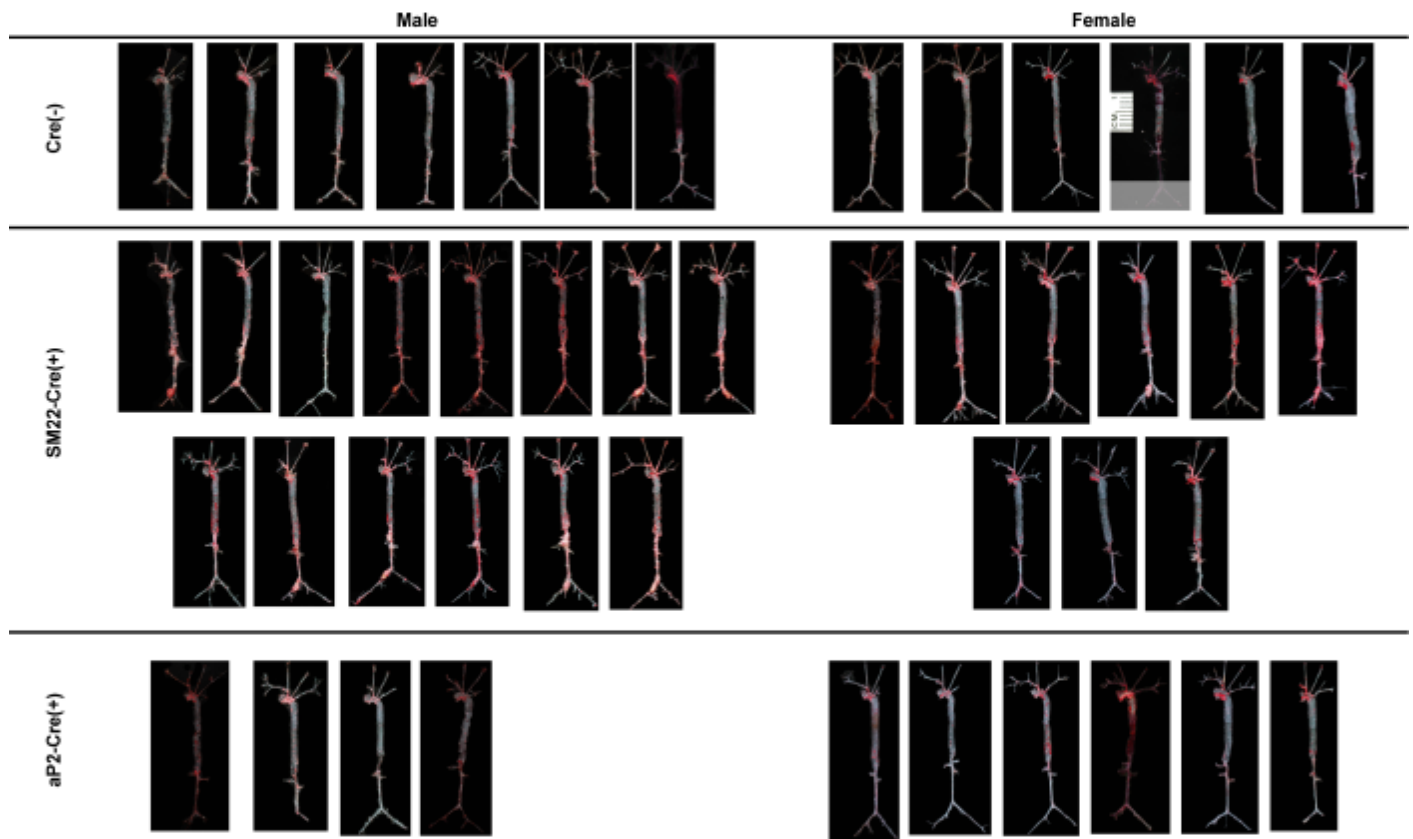


Figure S2. Gene expression of Acta2(α -SMA), Cre enzyme, MT1-MMP (MMP14), MMP2, MMP8, MMP9, MMP13, and MT2-MMP (MMP15) in primary VSMCs isolated from *Cre(-)* and *SM22 α -Cre(+)* *MMP14^{F/F}ApoE^{-/-}* mice. Almost complete suppression of MT1-MMP expression in primary VSMCs was confirmed coupled with SM22-dependent Cre expression. Expression of other MMPs was not affected. *** $P < 0.001$

